J. Fluid Mech. (1979), *vol.* 91, *part* 2, *pp.* 357–397
Printed in Great Britain

The linearized treatment of general forced gas oscillations in tubes

By PETER A. MONKEWITZ

Institute of Aerodynamics, Federal Institute of Technology (ETH), Zürich, Switzerland†

(Received 15 August 1977 and in revised form 29 June 1978)

A general linear theory is presented to describe oscillatory flows of gases and liquids in a tube of circular cross-section, including the effects of radial and tangential pressure gradients as well as the temperature. The basic equations are solved by separation of variables. The resulting eigenvalue equation is extensively discussed whereby the splitting of the eigenvalues into 'bands' is obtained in a natural way. A systematic analysis of a number of simplified cases leads to analytic approximations for the eigenvalues over an extended domain of parameter variation (frequency, friction) so that a complete survey of all the eigenvalues is established. Then the problem of satisfying simultaneously arbitrary end-conditions for all flow variables with the obtained bands of eigenfunctions is formulated in a way to allow the application of Galerkin's method. Finally the theory is applied to a few examples of 'end-layers' and radial resonance, which cannot be treated by previous theories.

1. Introduction

This paper deals in a most general way with forced steady-periodic linear gas oscillations in a rigid tube of circular cross-section with a finite or half-infinite axial extent. The oscillations are assumed to be driven by arbitrary steady-periodic boundary conditions at one of the tube ends (e.g. by a piston or a membrane). The geometry is thus given by figure 1.

Since Kirchhoff (1868) formulated the appropriate equations, including diffusive effects, the problem has received a great deal of attention (cf. the survey by Tijdeman 1975). A first class of closed form solutions which is characterized by the assumption of zero radial pressure gradient has been worked out by Iberall (1950), Bergh & Tijdeman (1965) and Rott (1969). The removal of this restriction and the determination of higher radial modes has been undertaken by Scarton (1970), Scarton & Rouleau (1973) for a compressible liquid contained in a tube and by Huerre & Karamcheti (1976) for a gas in a plane duct. The importance of this generalization is obvious when wavelengths of the order of the tube diameter or smaller are considered and or when the tube length is small. In the first case Rayleigh (1945, paragraphs 340, 349, 350) has already pointed out that radial resonances associated with large radial pressure gradients must be expected. In the second case of short tubes the 'endlayers' become important where the transition, again associated with radial pressure gradients, between the imposed end-condition and the dominating modes away from the ends

† Present address: Department of Aerospace Engineering, University of Southern California, Los Angeles.

0022-1120/79/4160-5940 $02.00

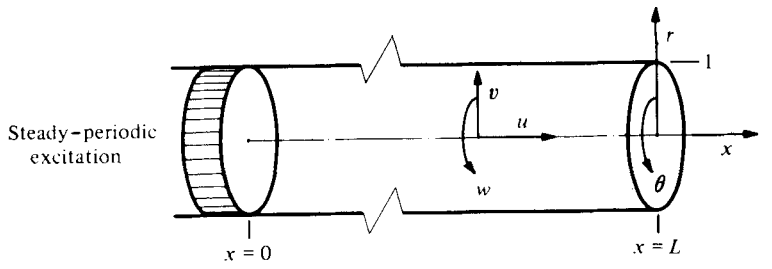

FIGURE 1. Situation and co-ordinates.

takes place. With the knowledge of the higher radial modes the problem of actually calculating a flow field with given end-conditions arises naturally, but so far the proper superposition of the modes has received surprisingly little attention: the results of Gerlach & Parker (1967) which used only modes with inviscid counterparts are reported by Scarton (1970) to be incorrect and an iterative scheme proposed by Scarton (1970) is shown in Monkewitz (1977) to be not generally applicable.

In the present study the work of Scarton (1970) is generalized to gas oscillations, i.e. temperature effects are included. The full linearized governing equations are solved by separation of variables which leads to a generalized eigenvalue equation (§§ 2 and 3). Thereby the non-axisymmetric modes have been retained in the analysis. In § 4 the eigenvalue equation is solved with special emphasis on analytical approximations for the eigenvalues in order to provide a picture of the radial and tangential modes over the whole range of parameter variation without referring to a computer program. Then the problem of satisfying simultaneously a complete set of end-conditions for the three velocity components and the temperature fluctuation is solved in § 5; the formulation in a suitably chosen 'endvector-space' makes the application of Galerkin's method possible. In order to obtain reasonable approximations with a restricted number of modes it is shown that the freedom of weighing the different end-conditions has to be built into the Hilbert space. Furthermore it is shown that for a given total number of modes there is an optimal relation between the number of modes from each band. In § 6 these methods are applied to several examples of 'endlayers' and of radial resonance, which cannot be treated by previous theories. In one particularly interesting case of radial resonance an approximate analytic solution for small frictional effects could be derived.

2. The linearized basic equations

Consider a compressible Newtonian fluid undergoing small amplitude motions. Each dependent variable such as pressure, density, velocity and temperature may be written in the form of a perturbation expansion:

$$q^*(r^*, \theta, x^*; t^*) = q_0^* + q_1^*(r^*, \theta, x^*; t^*) + q_2^*(r^*, \theta, x^*; t^*) + \ldots, \tag{2.1}$$

where q_0^* is a mean value over space and time and $q_1^*, q_2^*, \ldots$ designate fluctuating quantities of higher order. Assuming that there is no mean flow (i.e. $v_0^* = 0$), the coefficients of shear viscosity μ, bulk viscosity κ and heat conduction λ are constant to linear order and the first order (linearized) equations of continuity, motion, thermal energy and the equation of state are given by (2.2)–(2.5). It has to be noted that the

equation of state is specialized to the perfect gas equation with $R\,(=c_p-c_v)$ denoting the gas constant. This simplifies the following algebra but does not constitute a severe mathematical simplification as Huerre & Karamcheti (1976) derived under the sole assumption of local thermodynamic equilibrium a linearized equation of state which differs from (2.5) only in the coefficients of p_1^* and ρ_1^*.

$$\frac{1}{\rho_0^*}\frac{\partial \rho_1^*}{\partial t^*}+\operatorname{div}\mathbf{v}_1^*=0, \tag{2.2}$$

$$\rho_0^*\frac{\partial \mathbf{v}_1^*}{\partial t^*}=-\operatorname{grad}p_1^*+\mu\left[-\operatorname{curl}\operatorname{curl}\mathbf{v}_1^*+\left(\tfrac{4}{3}+\frac{\kappa}{\mu}\right)\operatorname{grad}\operatorname{div}\mathbf{v}_1^*\right], \tag{2.3}$$

$$\rho_0^* c_p\frac{\partial T_1^*}{\partial t^*}-\frac{\partial p_1^*}{\partial t^*}=\lambda\operatorname{div}\operatorname{grad}T_1^*, \tag{2.4}$$

$$T_1^*=\frac{1}{R\rho_0^*}p_1^*-\frac{T_0^*}{\rho_0^*}\rho_1^*. \tag{2.5}$$

These six scalar equations for the unknown quantities p_1^*, ρ_1^*, T_1^* and the three velocity components describe the fluid motion with good accuracy under the following assumptions:

(*a*) *Continuum hypothesis*: significant changes of dependent variables occur over distances large compared to the molecular scale given by the mean free path in a gas or the mean molecule spacing in a liquid.

(*b*) *The acoustic quantities* (index 1) *are small compared with their mean values* (index 0) *as are the higher order corrections compared with the acoustic quantities* thus justifying the linearization of the equations. The first part of the assumption can always be fulfilled by choosing the excitation amplitude of the oscillation small enough. The second part of the assumption is found to be in general a consequence of the first except in a few distinct cases which are: longitudinal resonances treated by Chester (1964) and Keller (1976), subharmonic resonances (cf. Keller 1975), most probably radial resonances and boundary conditions leading to large or singular second-order corrections (cf. discussion of b.c.).

(*c*) *Laminar motion*: Sergeev (1966) and Merkli & Thomann (1975) have shown that for the case of harmonic oscillations in a tube the motion is entirely laminar if the Reynolds number $Re=u_{\max}^*/(\nu\omega^*)^{\frac{1}{2}}$ based on the peak axial velocity $u_{\max}^*$ and the Stokes layer thickness $(\nu/\omega^*)^{\frac{1}{2}}$ is below its critical value of 150–350.

Introducing non-dimensional quantities† with the tube radius r_0^*, the mean sound speed a_0, the mean density ρ_0^*, $\rho_0^* a_0^2$ and a_0^2/c_p as reference length, velocity, density, pressure and temperature, and further introducing the scalar and vector potentials ϕ_1 and $\boldsymbol{\Psi}_1$, assuming that the time-dependence of all acoustic quantities is given by the factor $\exp(i\omega t)$ and using the relation $a_0^2=\gamma RT_0^*$ for the mean sound speed leads to the following set of equations:

$$\left[(\operatorname{div}\operatorname{grad})\boldsymbol{\Psi}_1-\frac{i\omega}{\Lambda}\boldsymbol{\Psi}_1\right]_r=0, \tag{2.6}$$

$$\left[(\operatorname{div}\operatorname{grad})\boldsymbol{\Psi}_1-\frac{i\omega}{\Lambda}\boldsymbol{\Psi}_1\right]_\theta=0, \tag{2.7}$$

$$\operatorname{div}\operatorname{grad}\phi_1(1+i\omega\Lambda\gamma\alpha)+\omega^2\gamma\phi_1-i\omega(\gamma-1)T_1=0, \tag{2.8}$$

† Dimensional quantities are denoted by *.

$$\operatorname{div}\operatorname{grad} T_1(1+i\omega\Lambda\gamma\alpha) - \frac{i\omega\sigma}{\Lambda}(1+i\omega\Lambda\alpha)T_1 + \frac{\omega^2\sigma}{\Lambda}\phi_1 = 0, \tag{2.9}$$

with ψ_{1x} given by $\operatorname{div}\boldsymbol{\Psi}_1 = 0,$ (2.10)

where $\gamma, \sigma, \alpha = \frac{4}{3} + (\kappa/\mu)$ and $\Lambda = \nu/a_0 r_0^*$ are the specific heat ratio, the Prandtl number, the non-dimensional bulk viscosity parameter and the friction parameter respectively. It must be noted that Λ is of the order of the ratio of mean free path and tube radius r_0^* for gases or of the ratio of mean molecule spacing and tube radius for common liquids such as water. Thus assumption (a) of this section implies $\Lambda \ll 1$ except for very viscous liquids which will not be considered.

The original first-order quantities are recovered through the relations:

$$\left.\begin{aligned} \mathbf{v}_1 &= \operatorname{grad}\phi_1 + \operatorname{curl}\boldsymbol{\Psi}_1, \\ \rho_1 &= -\frac{1}{i\omega}\operatorname{div}\operatorname{grad}\phi_1, \\ p_1 &= -i\omega\phi_1 + \Lambda\alpha \operatorname{div}\operatorname{grad}\phi_1. \end{aligned}\right\} \tag{2.11}$$

For the domain $0 \leqslant r \leqslant 1$ and $0 \leqslant x \leqslant L$ $(0 < L \leqslant \infty)$ the following boundary conditions on $\mathbf{v}_1$ and T_1 are considered (conditions on other variables such as pressure, which could easily be substituted, are not considered because of the difficulty of comparison with an experiment).

Condition on the tube axis: to exclude Neumann-type singular solutions every acoustic quantity q_1 has to fulfil the condition

$$q_1(r = 0, \theta, x; t) < \infty. \tag{2.12}$$

Boundary conditions at the tube perimeter: all velocity components and the temperature fluctuations are assumed to vanish at $r = 1$. This means that the tube wall is rigid and has a much larger heat capacity than the fluid.

$$\left.\begin{aligned} \mathbf{v}_1(r = 1, \theta, x; t) &= \mathbf{0}, \\ T_1(r = 1, \theta, x; t) &= 0. \end{aligned}\right\} \tag{2.13}$$

Boundary conditions at the tube ends: it is assumed that the displacement $x_w(r, t)$ of the end wall at $x = 0$ is given in the form of the Fourier series

$$x_w = \sum_{m=0}^{\infty} \hat{x}^{(m)}(r)\exp(im\theta + i\omega t), \tag{2.14}$$

whereas the end at $x = L$ is closed. Thus the axial velocity at the moving wall $u(x_w)$ is given by $\partial x_w/\partial t$ and the no-slip condition yields for the radial and tangential velocities v and w

$$u(x_w) : v(x_w) : w(x_w) = 1 : -\partial x_w/\partial r : -r^{-1}\partial x_w/\partial\theta.$$

Upon expanding into Taylor series around $x = 0$ and arranging the terms according to the perturbation expansion (2.1) the following end-conditions are obtained to linear order:

$$\left.\begin{aligned} u_1(r, \theta, x = 0; t) \equiv u_e &= \sum_{m=0}^{\infty} \hat{u}_e^{(m)}(r)\exp(im\theta + i\omega t), \\ v_1 = w_1 &= T_1(r, \theta, x = 0; t) = 0, \\ u_1 = v_1 = w_1 &= T_1(r, \theta, x = L; t) = 0, \end{aligned}\right\} \tag{2.15}$$

with the suitable normalization

$$\|\hat{u}_e^{(0)}(r)\|^2 \equiv \int_0^1 |\hat{u}_e^{(0)}(r)|^2 r\,dr = 1.$$

At this point it is also worth looking at the driving end-condition for the second-order quantities which are evaluated as:

$$\left.\begin{aligned} u_2(r,\theta,x=0;t) &= -x_w \frac{\partial u_1}{\partial x}\ (x=0), \\ v_2(r,\theta,x=0;t) &= -\frac{\partial x_w}{\partial r} u_e - x_w \frac{\partial v_1}{\partial x}\ (x=0), \\ w_2(r,\theta,x=0;t) &= -\frac{1}{r}\frac{\partial x_w}{\partial \theta} u_e - x_w \frac{\partial w_1}{\partial x}\ (x=0). \end{aligned}\right\} \tag{2.16}$$

To assure that the second-order excitation amplitudes are much smaller than the first-order amplitude $u_e = i\omega x_w$, the following conditions involving the linear solution $\mathbf{v}_1$ must hold:

$$\left|\frac{\partial x_w}{\partial r}\right| \ll 1, \quad \left|\frac{1}{r}\frac{\partial x_w}{\partial \theta}\right| \ll 1, \tag{2.17}$$

$$\left|\frac{1}{\omega}\frac{\partial \mathbf{v}_1}{\partial x}\ (x=0)\right| \ll 1. \tag{2.18}$$

These conditions have to be considered when designing an experiment where radial modes are important since the plane piston strikingly violates condition (2.18) thus indicating that nonlinear effects are essential in the corner between a moving piston and the wall.

3. The solution of the basic equations by separation of variables

In Monkewitz (1977), denoted hereafter as TH, plausibility arguments are given for the problem being well posed which are based on the strong ellipticity (cf. Nirenberg 1955) of the system of equations (2.6)–(2.9). Proceeding to the practical solution the trial solution

$$q = \sum_{m=0}^{\infty} \hat{q}^{(m)}(r) \exp(\pm Kx + im\theta + i\omega t), \tag{3.1}$$

is introduced for every acoustic variable q (omitting the index 1 in the following). The representation of q by a Fourier series in θ is justified by its periodicity; the separation of x and r on the other hand is possible as the x-dependence in all four equations (2.6)–(2.9) is given by the sole differential $\partial^2/\partial x^2$. This 'fortunate' fact constitutes the key to the analytic solution enabling the separation of all the four equations with the *same separation constant* K^2, K being referred to as 'axial wavenumber' or 'eigenvalue'.

The first two equations (2.6) and (2.7) are solved by setting $\hat{\Psi}_r^{(m)} = \Gamma \hat{\Psi}_\theta^{(m)}$ yielding a quadratic equation for Γ with the solutions $\Gamma = \pm i$. Taking into account the condition (2.12) the general solution for every order (m) of the θ Fourier series with suitably chosen constants C_u and C_w is found to be:

$$\hat{\Psi}_r^{(m)} = iC_u \frac{m}{M_u r} J_m(M_u r) + \tfrac{1}{2} iC_w [J_{m+1}(M_u r) - J_{m-1}(M_u r)], \tag{3.2}$$

$$\hat{\Psi}_y^{(m)} = \tfrac{1}{2}C_u[J_{m+1}(M_u r) - J_{m-1}(M_u r)] + C_w \frac{m}{M_u r} J_m(M_u r), \tag{3.3}$$

with J_m denoting the Bessel function of integer order m and the 'radial wave number' M_u given by

$$M_u = \pm \left[K^2 - \frac{i\omega}{\Lambda}\right]^{\frac{1}{2}}. \tag{3.4}$$

The third component $\hat{\Psi}_x^{(m)}$ is calculated through the relation (2.10):

$$\hat{\Psi}_x^{(m)} = -iC_w \frac{M_u}{K} J_m(M_u r). \tag{3.5}$$

The sign in (3.4) has to be chosen such that M_u equals K in the limit $\omega \to 0$. In the following the double signs will be omitted and *all wavenumbers* will be supposed to lie *in the right complex half-plane*. The symmetric solutions are easily recovered through the symmetry relation given in § 4.2.

The equations (2.8) and (2.9) are solved in an analogous way by setting $\hat{T}^{(m)} = \Omega\hat{\phi}^{(m)}$. This yields again a quadratic equation for Ω with the solutions:

$$\Omega_{v,t} = \frac{1}{2(\gamma-1)}\left\{\left[\frac{\sigma}{\Lambda} - i\omega(\gamma-\beta)\right] \mp \left[\left[\frac{\sigma}{\Lambda} - i\omega(\gamma-\beta)\right]^2 + 4(\gamma-1)\frac{i\omega\sigma}{\Lambda}\right]^{\frac{1}{2}}\right\}, \tag{3.6}$$

where β is defined by $\beta = \sigma\alpha$. With appropriately normalized constants C_v and C_t one has finally:

$$\hat{\phi}^{(m)} = C_v J_m(M_v r) + C_t \Omega_t^{-1} J_m(M_t r), \tag{3.7}$$

$$\hat{T}^{(m)} = C_v \Omega_v J_m(M_v r) + C_t J_m(M_t r), \tag{3.8}$$

the radial wavenumbers M_v and M_t being defined by:

$$M_v = \left[K^2 + \frac{\gamma\omega^2 - i\omega(\gamma-1)\Omega_v}{1 + i\omega\Lambda\gamma\alpha}\right]^{\frac{1}{2}}; \quad \mathrm{Re}\,[M_v] \geqslant 0, \tag{3.9}$$

$$M_t = \left[K^2 + \frac{\gamma\omega^2 - i\omega(\gamma-1)\Omega_t}{1 + i\omega\Lambda\gamma\alpha}\right]^{\frac{1}{2}}; \quad \mathrm{Re}\,[M_t] \geqslant 0. \tag{3.10}$$

4. The application of the boundary conditions at the tube perimeter: the eigenvalue equation and its solutions

4.1. *The eigenvalue equation*

The application of the boundary conditions (2.13) at $r = 1$ on $\hat{T}^{(m)}$ and $\hat{\mathbf{v}}^{(m)}$ obtained in § 3 leads to a system of linear homogeneous equations for the constants C_v, C_t, C_u and C_w. For a non-trivial solution the determinant has to vanish, which yields the eigenvalue equation:

$$\begin{aligned}\left(1 - \frac{\Omega_v}{\Omega_t}\right) K^2 J_m(M_v) J_m(M_t) J_{m+1}(M_u) \left[J_m'(M_u) + \frac{m}{M_u K^2}\frac{i\omega}{\Lambda} J_m(M_u)\right] \\ - M_v M_u J_{m+1}(M_v) J_m(M_t) J_m(M_u)\,[J_m'(M_u)] \\ + \frac{\Omega_v}{\Omega_t} M_t M_u J_m(M_v) J_{m+1}(M_t) J_m(M_u)\,[J_m'(M_u)] = 0.\end{aligned} \tag{4.1}$$

Introducing the function $\qquad F_m(z) = 2J_{m+1}(z)/zJ_m(z), \tag{4.2}$

a second form of (4.1) is given which, although singularities are introduced, will be useful for analytic approximation purposes as the function F_m is easier to deal with than are single Bessel functions.

$$\left(1-\frac{\Omega_v}{\Omega_t}\right) K^2 F_m(M_u)\left[F_m(M_u)+\frac{2m}{K^2}-\frac{4m}{M_u^2}\right]-M_v^2 F_m(M_v)\left[F_m(M_u)-\frac{2m}{M_u^2}\right]$$
$$+\frac{\Omega_v}{\Omega_t} M_t^2 F_m(M_t)\left[F_m(M_u)-\frac{2m}{M_u^2}\right]=0. \qquad (4.3)$$

It has to be noted that, for $m = 0$ and $\gamma \to 1$, (4.1) reduces to the eigenvalue equation for liquids given by Scarton & Rouleau (1973) as in this case Ω_v/Ω_t tends to zero.

4.2. *General considerations on the solutions of the eigenvalue equation*

Instead of adopting a numerical approach to the solution of the eigenvalue equation (4.1), analytic considerations will be pushed as far as possible. The following general considerations enable the solutions to be put into a systematic order.

First a useful *symmetry property* of (4.1) is readily verified: with the set of wave-numbers $(K, M_v(K), M_t(K), M_u(K))$ also the symmetric set $(-K, -M_v(K), -M_t(K), -M_u(K))$ is a solution of (4.1). Thus the search for solutions can be restricted to the right complex half-plane.

The next step in finding all the *eigenvalues* is the evaluation of their *number* using the argument that for arbitrary end-conditions the superposition of the eigensolutions should yield a unique final solution, taking for granted that the problem is mathematically well posed (cf. § 5.3). For the mathematical formulation it is convenient to introduce the notion of endvectors. From any solution vector $S^{(m)}$ which is in general a linear combination of eigenvectors the corresponding *endvector* $\mathscr{S}^{(m)}$ is constructed as follows:

$$S^{(m)} \equiv \begin{pmatrix} T \\ u \\ v \\ w \end{pmatrix}^{(m)} (r,x) \xrightarrow[\substack{\text{tube}\\ \text{length } L}]{} \mathscr{S}^{(m)} \equiv \begin{pmatrix} T(r,x=0) \\ T(r,x=L) \\ u(r,x=0) \\ u(r,x=L) \\ v(r,x=0) \\ v(r,x=L) \\ w(r,x=0) \\ w(r,x=L) \end{pmatrix}^{(m)} . \qquad (4.4)$$

It has to be noted that for the half-infinite tube only the axially damped eigenfunctions proportional to $\exp(-Kx)$ (with K in the right complex half-plane) have to be retained so that the even components of all endvectors vanish. Now we consider pure endvectors which are defined by having only one component different from zero. With this idea each of the eight possible end-conditions, which are functions of r, can be matched independently by superimposing a complete set of the corresponding pure endvectors with appropriate amplitudes. Thus the number of complete sets of pure endvectors has to equal the number of end-conditions. By the argument that it must be possible to obtain these pure endvectors from the eigen-endvectors by a linear transformation, it is concluded that for the present case of eight end-conditions *eight infinite sets or 'bands' of eigenvalues have to exist, four in the right half-plane and four symmetric bands in the left half-plane* according to the symmetry property of the eigenvalue equation.

The four pairs of bands will be denoted by the capital letters A to D, thus extending the notation of Scarton.

Knowing the number of eigenvalue bands, a selection of simplified problems is exploited in the way of a heuristic 'perturbation approach' in order to obtain first a characterization of each band and second rough estimates for the eigenvalues. The simplest problem (a) is the unrealistic but instructive inviscid case with heat conduction which is solved explicitly. The second problem ($b0$), characterized by $\gamma = 1$ and $m = 0$, has been solved by Scarton & Rouleau (1973) except for the temperature and tangential velocity modes which form the C- and D-band. Furthermore their results have been reformulated in terms of 'natural' wavenumbers which will be discussed subsequently. The last case (bm) extends Scarton's results to $m > 0$. For each case the following results are listed: the eigenvalue equation, its bands of solutions (band indices A to D, order index n within each band) and the corresponding eigenvectors whereby also results of the subsequent discussion are incorporated.

(a) $\mu = 0, \lambda \neq 0, \gamma = 1$

Eigenvalue equation: $$J_m(M_t)\, J'_m(M_v) = 0,$$

with $$M_t^2 = K^2 - \frac{i\omega\sigma}{\Lambda} \quad \left(\frac{\Lambda}{\sigma} = \frac{\lambda}{\rho_0^* a_0 r_0^* c_p}\right), \qquad M_v^2 = K^2 + \omega^2. \tag{4.5}$$

Bands of solutions:

$$\left.\begin{aligned} \{M_{v,An}\} &= \pm\{j'_{m,n}\} \quad (j'_{m,n} = n\text{th zero of } J'_m), \\ \{M_{t,Cn}\} &= \pm\{j_{m,n}\} \quad (j_{m,n} = n\text{th zero of } J_m). \end{aligned}\right\} \tag{4.6}$$

Eigenvectors:

$$\begin{pmatrix} T \\ u \\ v \\ w \end{pmatrix}_{An}^{(m)\pm} = \begin{pmatrix} \mp \dfrac{i\omega}{K_{An}(1 - i\omega\Lambda/\sigma)} \left[J_m(j'_{m,n} r) - J_m(j'_{m,n}) \dfrac{J_m(M_{t,An} r)}{J_m(M_{t,An})} \right] \\ \pm J_m(j'_{m,n} r) \\ \pm \dfrac{j'_{m,n}}{K_{An}} J'_m(j'_{m,n} r) \\ \pm \dfrac{1}{K_{An}} \dfrac{im}{r} J_m(j'_{m,n} r) \end{pmatrix} \exp[\pm K_{An} x],$$

with $$K_{An} = (j'^2_{m,n} - \omega^2)^{\frac{1}{2}},$$

$$M_{t,An} = \left(j'^2_{m,n} - \omega^2 - \frac{i\omega\sigma}{\Lambda}\right)^{\frac{1}{2}}, \tag{4.7}$$

and $$\begin{pmatrix} T \\ u \\ v \\ w \end{pmatrix}_{Cn}^{(m)\pm} = \begin{pmatrix} J_m(j_{m,n} r) \\ 0 \\ 0 \\ 0 \end{pmatrix} \exp[\pm K_{Cn} x],$$

with $$K_{Cn} = \left(j^2_{m,n} + \frac{i\omega\sigma}{\Lambda}\right)^{\frac{1}{2}}.$$

($b0$) $\mu \neq 0, \lambda \neq 0, \gamma = 1, m = 0$

Eigenvalue equation:

$$J_1(M_u)\, J_0(M_t) \{K^2 J_0(M_v) J_1(M_u) - M_v M_u J_1(M_v)\, J_0(M_u)\} = 0. \tag{4.8}$$

Bands of solutions:

$$\left.\begin{aligned} \{M_{v,An}\} &\approx \pm\{j'_{0,n}\}, \quad \{M_{u,Bn}\} \approx \pm\{j_{1,n}\}, \\ \{M_{t,Cn}\} &= \pm\{j_{0,n}\}, \quad \{M_{u,Dn}\} = \pm\{j_{1,n}\}. \end{aligned}\right\} \tag{4.9}$$

Eigenvectors:

$$\begin{pmatrix} T \\ u \\ v \\ 0 \end{pmatrix}_{An}^{(0)\pm} \begin{pmatrix} T \\ u \\ v \\ 0 \end{pmatrix}_{Bn}^{(0)\pm} \begin{pmatrix} J_0(j_{0,n}r) \\ 0 \\ 0 \\ 0 \end{pmatrix}_{Cn}^{(0)\pm} \begin{pmatrix} 0 \\ 0 \\ 0 \\ J_1(j_{1,n}r) \end{pmatrix}_{Dn}^{(0)\pm} \tag{4.10}$$

(bm) $\mu \neq 0$, $\lambda \neq 0$, $\gamma = 1$, $m > 0$

Eigenvalue equation:

$$J_m(M_t)\left\{K^2 J_m(M_v)\, J_{m+1}(M_u)\left[J'_m(M_u) + \frac{m}{M_u K^2}\frac{i\omega}{\Lambda} J_m(M_u)\right] - M_v M_u J_{m+1}(M_v) J_m(M_u)\,[J'_m(M_u)]\right\} = 0. \tag{4.11}$$

Bands of solutions:

$$\left.\begin{aligned} \{M_{v,An}\} &\approx \pm\{j'_{m,n}\}, \quad \{M_{u,Bn}\} \approx \pm\{j_{m-1,n}\}, \\ \{M_{t,Cn}\} &= \pm\{j_{m,n}\}, \quad \{M_{u,Dn}\} \approx \pm\{j'_{m,n}\}. \end{aligned}\right\} \tag{4.12}$$

Eigenvectors:

$$\begin{pmatrix} T \\ u \\ v \\ w \end{pmatrix}_{An}^{(m)\pm} \begin{pmatrix} T \\ u \\ v \\ w \end{pmatrix}_{Bn}^{(m)\pm} \begin{pmatrix} J_m(j_{m,n}r) \\ 0 \\ 0 \\ 0 \end{pmatrix}_{Cn}^{(m)\pm} \begin{pmatrix} T \\ u \\ v \\ w \end{pmatrix}_{Dn}^{(m)\pm}. \tag{4.13}$$

The main ideas for the solution of the more general eigenvalue equations can be extracted from the inviscid case (a), the primary result being the *'natural' characterization of bands*: each band of solutions (4.6) is obviously characterized by a specific radial wavenumber – the natural wavenumber of the band – which takes finite values irrespective of the parameters ω and Λ/σ. So the *A-band is characterized by* M_v which takes the finite values $j'_{m,n}$ while K_{An} and $M_{t,An}$ are not limited to a finite region of the complex plane as $\omega \to \infty$; in the same way the *C-band is characterized by* M_t which takes the values $j_{m,n}$ while K_{Cn} is not bounded as $\omega \to \infty$. This idea carries over to the more general eigenvalue equations in the following way: the natural wavenumbers for each band are confined to finite regions of the complex wavenumber-plane independently of all parameters whereby for different orders n within a band these regions are separated in an unambiguous way. These features which are essential for analytic approximations as well as for a simple numerical search procedure, are associated only with the natural radial wavenumbers which are functions of the original eigenvalue K. Therefore the solution of the eigenvalue equation for each band is most conveniently sought in terms of its natural wavenumber.

A further point of attention is the appearance of pure solutions, i.e. eigenvectors with only one component different from zero, which is associated with the decoupling of one of the basic equations. In case (a) with $\gamma = 1$ the pure T-solution stems from the decoupled thermal energy equation.

The above results are now carried over to the more complex case (b). The physical argument that the case (b) cannot be fundamentally different from the inviscid case (a) at least for small friction effects suggests the natural *A-band* eigenvalues $M_{v,An}$ to

lie in the neighbourhood of the inviscid solutions $j'_{m,n}$. By the consideration of the limiting solutions $\omega \to 0$ and $\omega \to \infty$ (Λ fixed) in §§4.4 and 4.5 this idea is proved to be correct even for arbitrary friction effects and $\gamma \neq 1$; the only exception is found to be the solution $M_{v,A1}$ which departs significantly from $j'_{m,1}$ at high frequency, but it is proved that $M_{v,A1}$ is still finite in the limit $\omega \to \infty$ so that the concept of the natural wavenumber remaining finite is fully confirmed for the *A*-band. With the *C-band* no problem occurs in case (*b*) as the basic equations accept a pure T-solution for $\gamma = 1$. The new feature in case (*b*) is the possibility of satisfying homogeneous boundary conditions at $r = 1$ not only for T and v but also for u and w. This gives rise to two new bands – the *B*- and *D*-band – which have both to be characterized by the new wavenumber M_u. For the case (*b*0) the rough estimate (4.9) for the *B-band* solutions is obtained by recasting the results of Scarton & Rouleau (1973) in terms of the natural wavenumber $M_{u,Bn}$ whereas the *D-band* solutions are obtained as zeroes of the factor $J_1(M_u)$ in the eigenvalue equation (4.8) and represent pure w-solutions. For the case (*bm*) the estimate (4.12) for the *D*-band is then suggested by the form of the eigenvalue equation (4.11) while the estimates for the other bands remain unchanged.

At this point the step to the solution of the most general eigenvalue equation (4.1) is reduced to the removal of the restriction $\gamma = 1$ in the case (*b*). With $\gamma \neq 1$ the oscillation undergoes an additional 'temperature damping'. As the estimates (4.9) and (4.12) are found to be independent of friction effects it is conjectured that likewise they are not affected by this additional damping. The argument is also supported by the fact that the eigenvalues have to depend continuously on γ. The principal difference to case (*b*) lies in the *C-band* being no longer a pure temperature band. But as Ω_v/Ω_t is of the order $(\gamma - 1)\Lambda$ (cf. §4.3) the first two terms in (4.1) containing the factor $J_m(M_t)$ dominate the third term in the measure that $j_{m,n}$ remains a good estimate for $M_{t,Cn}$.

Herewith the solutions of the eigenvalue equation (4.1) are completely systematized and rough estimates are established. In the remainder it is proved in detail that all the natural wavenumbers remain finite in both limits $\omega \to 0$ and $\omega \to \infty$. In addition, useful intermediate approximations are obtained so that a complete survey of the behaviour of all eigenvalues results. The quick reader may skip the following details and proceed directly to §4.6 where the physics of the solutions is discussed.

4.3. *The choice of suitable expansion parameters*

The formulation of the continuum hypothesis in terms of the actual parameters of the problem yields four quantities, which have to be kept small compared to unity: the first is the friction parameter Λ which is shown in §2 to be of the order of the ratio of the molecular scale and the tube diameter. The second is the quantity $\omega\Lambda$ which is found analogously to be of the order of the ratio of the molecular scale and the wavelength a_0/ω^*. If on the other hand the molecular scale is compared to a 'radial wavelength' r_0^*/n, which is the approximate radial spacing between the nodes of an nth order inviscid eigensolution, the third quantity $n\Lambda$ is obtained; finally the comparison of the molecular scale with a 'tangential wavelength' $1/m$ ($m > 0$) yields the fourth quantity $m\Lambda$. The conditions imposed by the continuum hypothesis – $\Lambda \ll 1$, $\omega\Lambda \ll 1$, $n\Lambda \ll 1$, $m\Lambda \ll 1$ – represent a restriction on the geometry and the material constants and as soon as Λ is fixed, a cutoff for the frequency ω, the radial mode order n and the tangential order m. For the following expansion purposes, ϵ defined by (4.14) is chosen as the most convenient small expansion parameter. As a second parameter, the

inverse non-dimensional Stokes layer thickness η is chosen, as it is widely used in the literature.

$$\epsilon = -i\omega\Lambda; \quad \eta = \left(\frac{i\omega}{\Lambda}\right)^{\frac{1}{2}} \quad (Re[\eta] \geqslant 0). \tag{4.14}$$

Upon expanding with respect to ϵ, the quantities Ω_v, Ω_t and the wavenumbers M_v, M_t, M_u are given by:

$$\left.\begin{aligned} \Omega_v &= \frac{\epsilon}{\Lambda}\left\{1+\left(\frac{\epsilon}{\sigma}\right)(\beta-1)+(\beta-1)\,O(\epsilon^2)\right\}, \\ \Omega_t &= \frac{\sigma}{(\gamma-1)\Lambda}\left\{1-\left(\frac{\epsilon}{\sigma}\right)(\beta-1)+(\beta-1)\,O(\epsilon^2)\right\}, \\ \frac{\Omega_v}{\Omega_t} &= \epsilon\frac{\gamma-1}{\sigma}\left\{1+2\left(\frac{\epsilon}{\sigma}\right)(\beta-1)+(\beta-1)\,O(\epsilon^2)\right\}. \end{aligned}\right\} \tag{4.15}$$

$$\left.\begin{aligned} M_v^2 &= K^2+\eta^2\epsilon\left\{1+\left(\frac{\epsilon}{\sigma}\right)(\gamma+\beta-1)+O(\epsilon^2)\right\}, \\ M_t^2 &= K^2-\eta^2\sigma\left\{1+\left(\frac{\epsilon}{\sigma}\right)(\gamma-1)(\beta-1)+(\gamma-1)(\beta-1)\,O(\epsilon^2)\right\}, \\ M_u^2 &= K^2-\eta^2. \end{aligned}\right\} \tag{4.16}$$

4.4. *The limit $\omega \to 0$ for the eigenvalues*

In the limit $\omega \to 0$ all radial wavenumbers tend to K so that in this case one has only to deal with a single eigenvalue K. To derive the *limiting eigenvalue equation for* K the expansions (4.15) and (4.16) up to terms proportional to ω, i.e. proportional to η^2 or ϵ are introduced in the general eigenvalue equation (4.1). Expanding all Bessel functions around K and introducing the function F_m already defined by (4.2) together with its derivative yields the result:

$$J_m(K)\left\{J'_m(K)\,F'_m(K)-\frac{2m}{K^2}\,J_m(K)\,F_m(K)\right\} = 0, \tag{4.17}$$

with

$$F'_m(z) = \frac{2}{z}-\frac{2(m+1)}{z}\,F_m(z)+\frac{z}{2}\,F_m^2(z).$$

The simplest solution of (4.17) which is identified as limiting *C-band* solution is obtained when setting $J_m(K) = 0$:

$$M_{t,\,Cn}(\omega = 0) = K_{Cn}(\omega = 0) = j_{m,\,n}, \quad n = 1, 2, \ldots. \tag{4.18}$$

A further solution is obtained with the asymptotic trial solution for large n,

$$K = j'_{m,\,n}+cj'^{-3}_{m,n}+O(j'^{-5}_{m,\,n}).$$

Introducing this expression into the curly brackets of (4.17) and expanding into negative powers of $j'_{m,\,n}$ yields $c = -2m^2$. For small n a computer calculation and the limiting solution (4.29) for $\omega \to \infty$ show that the first solution of (4.17) of this kind is only found in the neighbourhood of the second zero of J'_m. Thus the following approximations are found for these solutions which constitute the limiting *D-band* solutions:

$$M_{u,\,Dn}(\omega = 0) = K_{Dn}(\omega = 0) = j'_{m,\,n+1}-\frac{2m^2}{j'^3_{m,\,n+1}}+O\left(\frac{m^4}{j'^5_{m,\,n+1}}\right), \quad n = 1, 2, \ldots. \tag{4.19}$$

In table 1 the approximations (4.19) are compared to the computer calculations whereby two comments have to be made: the first concerns the solutions for $m = 0$

n	$m = 0$	$m = 1$
1	3·83171	5·31725 (5·31824)
2	7·01559	8·53301 (8·53310)
3	10·17347	11·70474 (11·70475)
4	13·32369	14·86297 (14·86297)
5	16·47063	18·01518 (18·01518)
n	$m = 2$	$m = 8$
1	6·67409 (6·67960)	14·01628 (14·07001)
2	9·96070 (9·96140)	17·73812 (17·75121)
3	13·16670 (13·16687)	21·21088 (21·21568)
4	16·34564 (16·34569)	24·57642 (24·5/859)
5	19·51181 (19·51183)	27·88226 (27·88337)

TABLE 1. Comparison of the exact values of $M_{u,\,D_n}(\omega = 0)$ with the approximated values (between parentheses) given by (4.19).

which are shown in § 4.2 to be exact over the whole parameter range; second, some decline of agreement is observed at $m > n$ which is explained by $j'_{m,\,n+1}$ being asymtotically equal to m for $m \gg n$.

The remaining limiting solutions of (4.17) for the *A- and B-band* are obtained by the asymptotic trial solution for large $|K_0|$, $K = K_0 + c_1 K_0^{-1} + c_2 K_0^{-2} + O(K_0^{-3})$ where K_0 is implicitly defined by $F'_m(K_0) = 0$. This series is introduced into the curly brackets of (4.17) whereby $F_m(K_0)$ can be expressed as a function of K_0 using $F'_m(K_0) = 0$. Upon expanding into negative powers of K_0 one finds:

$$K = K_0 + mK_0^{-1} \pm 2imK_0^{-2} + O(K_0^{-3}) \quad \text{with} \quad F'_m(K_0) = 0. \tag{4.20}$$

It remains to find the solutions K_0 of $F'_m(K_0) = 0$ or of the equivalent equation:

$$J_m^2(K_0) + J_{m+1}^2(K_0) - \frac{2(m+1)}{K_0} J_m(K_0) J_{m+1}(K_0) = 0. \tag{4.21}$$

This equation (4.21) has already been solved numerically and asymptotically by Scarton (1970) and Fitz-Gerald (1972) for $m = 0$. Here a generalized and improved asymptotic solution of (4.21) is presented. Using Hankel's asymptotic expansions for the Bessel functions (cf. Abramowitz & Stegun, 1969, equation 9.2.5) (4.21) is asymptotically equal to:

$$1 + \frac{(-1)^m}{2K_0}\cos(2K_0) - \frac{4\bar{m}^2 - 1}{2(2K_0)^2}[(-1)^m \sin(2K_0) + 1] - \frac{(-1)^m (4\bar{m}^2 - 1)(4\bar{m}^2 - 9)}{8(2K_0)^3}\cos(2K_0) + O(K_0^{-4}) = 0 \quad \text{with} \quad \bar{m} = m + 1. \tag{4.22}$$

Now it is obvious that for a solution to exist, $\cos(2K_0)$ must be of the order K_0 and consequently $\sin(2K_0)$ of the order unity. This is achieved by putting:

$$\left.\begin{aligned} 2K_0 &= x + iy, \\ x &= x_0\left\{1 + \frac{x_1}{x_0^2} + \ldots\right\}; \quad x_0 = (2n + m - 1)\pi, \\ y &= \pm \ln\left[x_0 y_0 \left(1 + \frac{y_1}{x_0^2} + \ldots\right)\right] = \pm\left\{\ln(x_0 y_0) + \frac{y_1}{x_0^2} + \ldots\right\}. \end{aligned}\right\} \tag{4.23}$$

n	$m=0$	$m=1$
1	0	$2{\cdot}56782-i1{\cdot}12261$
	(0)	$(2{\cdot}66166-i1{\cdot}20574)$
2	$4{\cdot}46630-i1{\cdot}46747$	$6{\cdot}00384-i1{\cdot}60811$
	$(4{\cdot}47703-i1{\cdot}46560)$	$(6{\cdot}01564-i1{\cdot}60894)$
3	$7{\cdot}69410-i1{\cdot}72697$	$9{\cdot}23221-i1{\cdot}81687$
	$(7{\cdot}69650-i1{\cdot}72653)$	$(9{\cdot}23566-i1{\cdot}81680)$
4	$10{\cdot}87457-i1{\cdot}89494$	$12{\cdot}41737-i1{\cdot}96127$
	$(10{\cdot}87544-i1{\cdot}89479)$	$(12{\cdot}41881-i1{\cdot}96120)$
5	$14{\cdot}03889-i2{\cdot}02006$	$15{\cdot}58564-i2{\cdot}07264$
	$(14{\cdot}03928-i2{\cdot}02000)$	$(15{\cdot}58636-i2{\cdot}07260)$
n	$m=2$	$m=8$
1	$3{\cdot}91454-i1{\cdot}31187$	$10{\cdot}91990-i1{\cdot}87859$
	$(4{\cdot}05261-i1{\cdot}41771)$	$(11{\cdot}77575-i2{\cdot}02281)$
2	$7{\cdot}41571-i1{\cdot}71396$	$14{\cdot}99089-i2{\cdot}12515$
	$(7{\cdot}44186-i1{\cdot}71757)$	$(15{\cdot}34379-i2{\cdot}13255)$
3	$10{\cdot}68450-i1{\cdot}89262$	$18{\cdot}59160-i2{\cdot}21989$
	$(10{\cdot}69355-i1{\cdot}89300)$	$(18{\cdot}78102-i2{\cdot}21856)$
4	$13{\cdot}89365-i2{\cdot}02015$	$22{\cdot}02415-i2{\cdot}29233$
	$(13{\cdot}89781-i2{\cdot}02017)$	$(22{\cdot}13967-i2{\cdot}29013)$
5	$17{\cdot}07777-i2{\cdot}12073$	$25{\cdot}37119-i2{\cdot}35376$
	$(17{\cdot}08002-i2{\cdot}12070)$	$(25{\cdot}44742-i2{\cdot}35183)$

TABLE 2. Comparison of the exact values of $M_{v,An}(\omega=0)=\overline{M_{u,Bn}(\omega=0)}$ with the approximated values (between parentheses) given by (4.24).

Upon introducing the above trial solution into (4.23) and expanding in powers of x_0^{-2} one finds consecutively y_0, x_1 and y_1. Inserting the resulting K_0 into (4.20) a pair of complex conjugate solutions for K are found for every m and n. By inspection of the high frequency approximations (4.33) and (4.39) or by a computer calculation the solutions with negative imaginary part are identified as the limiting A-band solutions, the corresponding complex conjugate solutions as the limiting B-band solutions.

$$\left.\begin{aligned} M_{v,An}(\omega=0)=K_{An}(\omega=0)\simeq\frac{1}{2}\left\{x_0-\frac{4m^2+3+2\ln(2x_0)}{2x_0}\right\}\\ -\frac{i}{2}\left\{\ln(2x_0)-\frac{32m^2+25-2(4m^2+1)\ln(2x_0)-2\ln^2(2x_0)}{(2x_0)^2}\right\},\\ x_0=(2n+m-1)\pi;\quad n=1,2,\ldots. \end{aligned}\right\} \tag{4.24}$$

$$M_{u,Bn}(\omega=0)=K_{Bn}(\omega=0)=\overline{M_{v,An}(\omega=0)}. \tag{4.25}$$

As for $m=0$, (4.17) has the exact solution $K=K_0=0$, the above approximation (4.24) is not appropriate for $(m,n)=(0,1)$. On the other hand the correspondence with computer calculations is remarkable in all other cases. This is shown in table 2 where again the quality of the approximation for higher m can be evaluated in the case $m=8$.

At this point all limiting solutions for $\omega=0$ have been obtained, with the A- and C-band solutions in the neighbourhood of their inviscid limits as anticipated in § 4.2. In a next step, the natural wavenumbers of each band could be expanded into power series in η^2 and ϵ around their limiting values, whereby in most of the cases the terms

proportional to ϵ can be safely neglected as $|\eta^2|$ is much larger than $|\epsilon|$. This would lead in the terminology of Huerre & Karamcheti (1976) to *low frequency* approximations which are limited in the case $(m,n) = (0,1)$ by $|\eta^2| < O(1)$ and in the other cases $(m,n) \neq (0,1)$ by $|\eta|^2 < O(|K^2(\omega = 0)|)$ thus extending the low frequency range of Huerre & Karamcheti to be dependent of m and n. Such approximations are carried out in the appendix of TH for the case $m = 0$ but as their practical use is very restricted, they are not incorporated in this paper.

4.5. *The limit $\omega \to \infty$ and high frequency approximations for the eigenvalues*

The proof that the natural wavenumbers remain finite over the whole parameter range is completed if the limiting solutions for $\omega \to \infty$ are also shown to be finite. For this mathematically interesting limit the unphysical *ultrahigh frequency range* characterized by $|\epsilon| \gg 1$ has to be considered, in which the continuum hypothesis is violated.

To find the solutions of the eigenvalue equation (4.3) in this range, the expansions (4.15) and (4.16) for the wavenumbers in terms of ϵ ($|\epsilon| \ll 1$) have to be replaced by the following expansions in terms of negative powers of ω (Λ fixed):

$$\left.\begin{aligned} \frac{\Omega_v}{\Omega_t} &\propto \frac{\sigma(\gamma-1)}{-i\omega\Lambda(\gamma-\beta)^2} + O(\omega^{-2}), \\ M_v^2 &\propto K^2 - \frac{i\omega}{\Lambda\alpha} + O(1), \\ M_t^2 &\propto K^2 - \frac{i\omega\sigma}{\Lambda\gamma} + O(1), \\ M_u^2 &= K^2 - \frac{i\omega}{\Lambda}, \end{aligned}\right\} \quad |\epsilon| \gg 1. \tag{4.26}$$

Furthermore the asymptotic expansion for $F_m(z)$ (cf. Abramowitz & Stegun 1969, equation 9.7.1) is needed:

$$F_m(z) \propto \pm \frac{2i}{z} + \frac{2m+1}{z^2} + O(z^{-3}), \quad |z| \gg 1, \quad |\arg[\mp iz]| < \tfrac{1}{2}\pi. \tag{4.27}$$

Proceeding in the same order as in § 4.4, first the trial solution $M_{t,Cn} = j_{m,n} + \delta$ for the limiting *C-band* solutions is made according to § 4.2. Then all other wavenumbers are expressed as functions of $M_{t,Cn}$ whereby all signs are evaluated with the material constants of air which does not affect the limit $j_{m,n}$. Using (4.27) and introducing all expansions into the eigenvalue equation (4.3) one finds:

$$M_{t,Cn} = j_{m,n}\left\{1 - \frac{\sigma(\gamma-1)}{\eta^3\Lambda^2(\gamma-\beta)^2}\left[\left(\frac{1}{\alpha}-\frac{\sigma}{\gamma}\right)^{\frac{1}{2}} + \frac{\sigma}{\gamma}\left(1-\frac{\sigma}{\gamma}\right)^{-\frac{1}{2}}\right]^{-1} + \ldots\right\}$$

$$\text{for} \quad |\epsilon| \gg 1 \quad \text{(ultrahigh frequency range)}$$

$$\lim_{\omega\to\infty} M_{t,Cn} = j_{m,n}. \tag{4.28}$$

As both limiting solutions (4.18) and (4.28) are identical and as in the same way $M_{t,Cn} \simeq j_{m,n}$ can be shown to be correct in all intermediate frequency ranges, it is concluded that the $j_{m,n}$ are always good approximations for the C-band solutions.

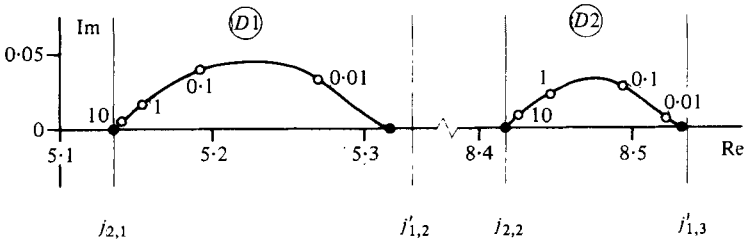

FIGURE 2. Plot of $M_{u,Dn}$ ($n = 1, 2$) in the complex $M_{u,Dn}$ plane for $m = 1$, $\gamma = 1$, $\alpha = \frac{4}{3}$ and $\Lambda = 10^{-4}$ with ω as parameter (● limiting solutions $\omega = 0$ and $\omega \to \infty$).

The limiting *D-band* solutions for $\omega \to \infty$ are next found in the neighbourhood of the limits (4.19) for $\omega = 0$ by the trial solution $M_{u,Dn} = j_{m+1,n} + c/\eta + O(\eta^{-2})$. Expressing again all wavenumbers in terms of the natural wavenumber $M_{u,Dn}$ one finds with (4.26) and (4.27) the following solution of the eigenvalue equation (4.3) for the ultrahigh frequency range:

$$M_{u,Dn} = j_{m+1,n}\left\{1 + \frac{i}{2\eta}\left(1 - \frac{1}{\alpha}\right)^{\frac{1}{2}} + \ldots\right\} \quad \text{for} \quad m > 0;$$

$$|\epsilon| \gg 1 \quad \text{(ultrahigh frequency range)},$$

$$\lim_{\omega \to \infty} M_{u,Dn} = j_{m+1,n}. \tag{4.29}$$

Going through the same procedure but using the expansions (4.15) and (4.16) for $|\epsilon| \ll 1$ instead of (4.26), also an approximation for $M_{u,Dn}$ in the high to very high frequency range (following the terminology of Huerre & Karamcheti 1976) is obtained.

$$M_{u,Dn} = j_{m+1,n}\left\{1 + \frac{i}{2\eta} + O(\eta^{-2})\right\} \quad \text{for} \quad m > 0;$$

$$|\epsilon| \ll 1, \quad \left|\frac{j_{m+1,n}}{\eta}\right| \ll 1 \quad \text{(high and very high frequency range)}. \tag{4.30}$$

Herewith the assertions of § 4.2 are also confirmed for the *D*-band as both limiting solutions $\omega = 0$ and $\omega \to \infty$ are finite although they are no longer identical like in the *C*-band; they only coalesce asymptotically as $j'_{m,n+1} \propto j_{m+1,n} \propto (n + \frac{1}{2}m + \frac{1}{4})\pi$ for $n \to \infty$ and m fixed. An example of the typical behaviour of $M_{u,Dn}$ between the limiting solutions is shown in figure 2 whereby also the approximation (4.30) is confirmed.

The form of the limiting *A-band* solutions is found by the following consideration: if $M_{v,An}$ is finite one finds with (4.26) and (4.27) that $K^2_{An} F_m(M_{u,An})$ in the eigenvalue equation (4.3) is proportional to η. Therefore $F_m(M_{v,An})$ has also to be proportional to η which yields $M_{v,An} = j_{m,\bar{n}} + c/\eta + O(\eta^{-2})$ with $F_m(M_{v,An}) = -2\eta/(c j_{m,\bar{n}}) + O(1)$. In the usual way the solution (4.31) is then obtained in which the connexion between n and $\bar{n}$ is left open for the following discussion.

$$M_{v,An} = j_{m,\bar{n}}\left\{1 - \frac{1}{\eta}\alpha\left(1 - \frac{1}{\alpha}\right)^{\frac{1}{2}} + \ldots\right\}$$

$$\text{for} \quad |\epsilon| \gg 1 \quad \text{(ultrahigh frequency range)}. \tag{4.31a}$$

The connexion between n and $\bar{n}$ is best elucidated by the computer calculation shown in figure 3 in which the effect of reducing systematically the value of Λ is studied;

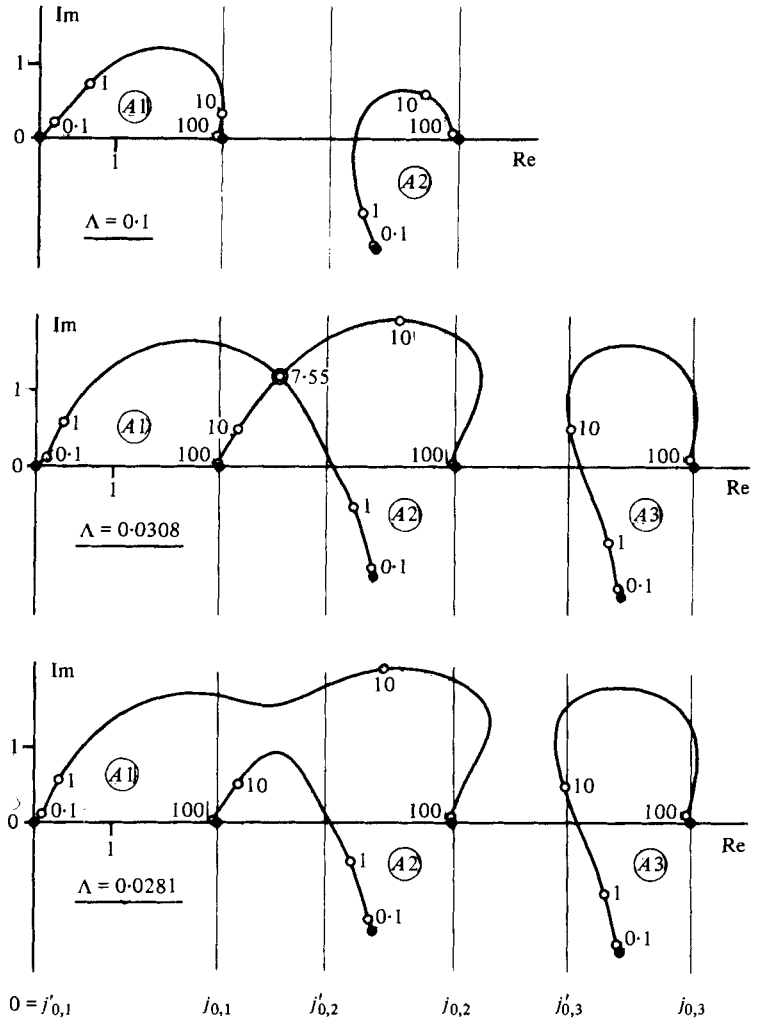

FIGURE 3. $M_{v,An}$ ($n = 1, 2, 3$) for $m = 0$, $\gamma = 1$, $\alpha = \frac{4}{3}$ and different Λ with ω as parameter (● limiting solutions $\omega = 0$ and $\omega \to \infty$).

thereby the special choice $\gamma = 1$, which does not affect the general behaviour of $M_{v,An}$, is motivated by the ultrahigh frequency range being only of interest for extremely viscous liquids. With this study one finds that $M_{v,A1}$ jumps successively to higher limiting values $j_{m,\bar{n}}$ as Λ is reduced and that at this specific $\bar{n}$ the character of the solution $M_{v,An}$ changes to give room to $M_{v,A1}$. In TH it is shown that this behaviour is essentially the same for all orders m so that the result (4.31*a*) is completed by:

$$\left.\begin{aligned} &\lim_{\omega\to\infty} M_{v,A1} = j_{m,\bar{n}} \quad \text{with} \quad \bar{n} = O\left(\frac{1}{10\Lambda\alpha}\right), \\ &\lim_{\omega\to\infty} M_{v,An} = j_{m,n-1} \quad \text{for} \quad 1 < n \leqslant \bar{n}, \\ &\lim_{\omega\to\infty} M_{v,An} = j_{m,n} \quad \text{for} \quad n > \bar{n}. \end{aligned}\right\} \tag{4.31b}$$

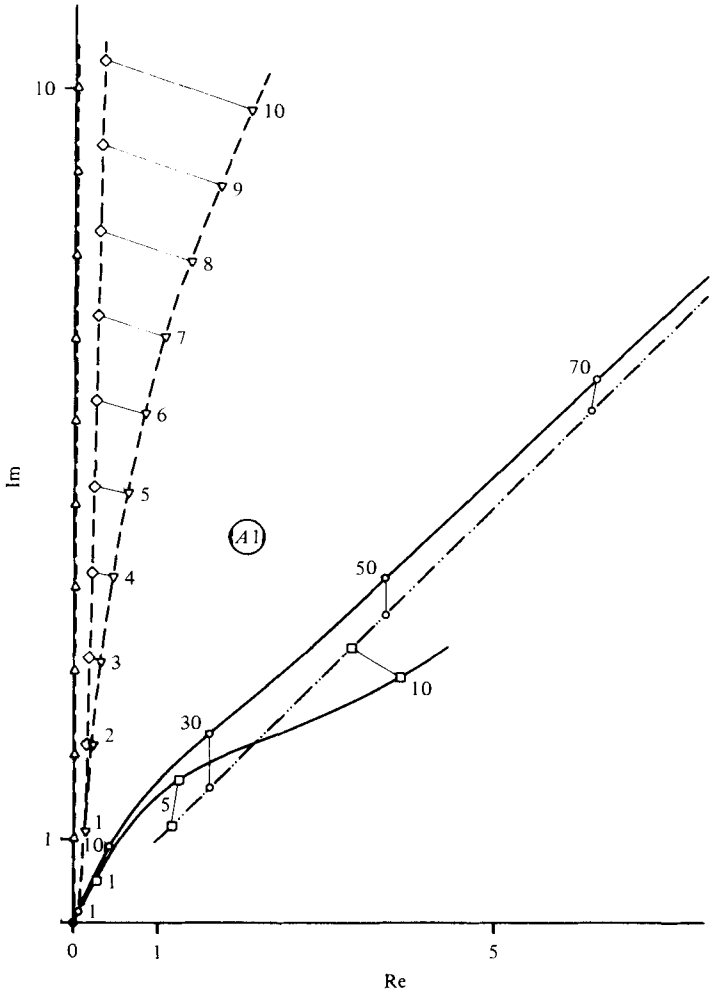

FIGURE 4. $M_{v,A1}$ and K_{A1} for $m = 0$, $\gamma = 1{\cdot}4$, $\sigma = 0{\cdot}71$, $\alpha = \frac{4}{3}$ and two different Λ with ω as parameter (● limiting solution $\omega = 0$). $\Lambda = 10^{-2}$: —□—, $M_{v,A1}$; – –▽– –, K_{A1}; – –◇– –, K_{BT} (Bergh & Tijdeman 1965). $\Lambda = 10^{-4}$: —○—, $M_{v,A1}$; – –△—, K_{A1}. Approximation (4.34) —··—.

Again one finds by using the expansions (4.15) and (4.16) instead of (4.26) approximations for the high frequency range:

$$M_{v,A1} = i\left[2\eta\epsilon\left(1+\frac{\gamma-1}{\sigma^{\frac{1}{2}}}\right)\right]^{\frac{1}{2}} + \ldots$$

for $|\eta| \gg 1$, $|\eta\epsilon| \ll 1$ (high frequency range) and $(m,n) = (0,1)$, (4.32)

$$M_{v,An} = j'_{m,n}\left\{1+\frac{1}{\eta}+\ldots\right\} - \eta\epsilon\,\frac{j'_{m,n}}{j'^{2}_{m,n}-m^2}\left(1+\frac{\gamma-1}{\sigma^{\frac{1}{2}}}\right)+\ldots$$

for $\left|\frac{j'_{m,n}}{\eta}\right| \ll 1$, $\left|\eta\epsilon\,\frac{j'_{m,n}}{j'^{2}_{m,n}-m^2}\right| \ll 1$ (high frequency range) and $(m,n) \neq (0,1)$. (4.33)

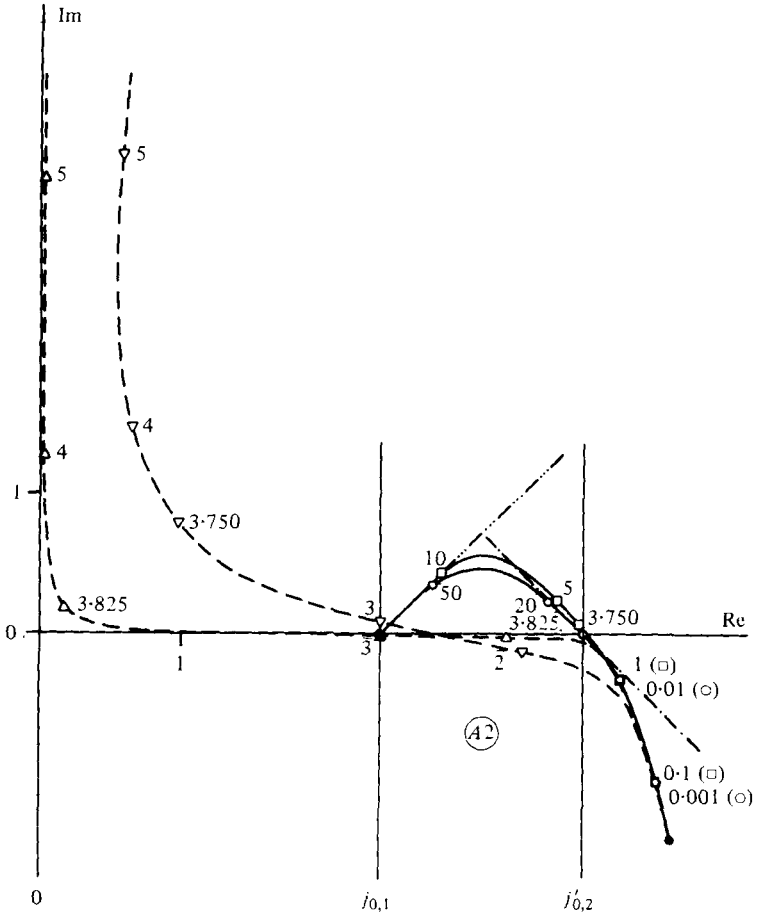

FIGURE 5. $M_{v,A2}$ and K_{A2} for $m = 0$, $\gamma = 1{\cdot}4$, $\sigma = 0{\cdot}71$, $\alpha = \frac{4}{3}$ and two different Λ with ω as parameter (● limiting solutions $\omega = 0$ and $\omega \to \infty$). $\Lambda = 10^{-2}$: —□—, $M_{v,A2}$; --▽--, K_{A2}. $\Lambda = 10^{-4}$: —○—, $M_{v,A2}$; --△--, K_{A2}. Approximations: —·— (4.33); —···— (4.35).

It has to be noted that (4.33) constitutes an expansion around the inviscid solutions $j'_{m,n}$ which is certainly valid for $\omega \simeq j'_{m,n}$ if Λ is sufficiently small to ensure that (4.33) is valid. With $\omega \simeq j'_{m,n}$ one finds then $K^2_{An} \simeq M^2_{v,An} - \omega^2 \simeq 0$ (cf. 4.5 and 4.16) so that the frequencies $\omega \simeq j'_{m,n}$ are identified as the radial resonance frequencies. This becomes obvious when looking at the inviscid A-band eigenvectors (4.7) and at the corresponding general expressions given in the appendix: a small excitation of the u_{An} component produces a large v_{An} component proportional to K^{-1}_{An}. Therefore this approximation (4.33) will be of primary importance for the analytic treatment of radial resonances in § 6.1.

Apart from the high frequency approximation (4.33), two further A-band solutions for the very high frequency range are found by the same procedure:

$$M_{v,A1} = i\eta\epsilon\left(1 + \frac{\gamma - 1}{\sigma^{\frac{1}{2}}}\right) + \ldots \quad \text{for} \quad |\epsilon| \ll 1,\ |\eta\epsilon| \gg 1$$

(very high frequency range), (4.34)

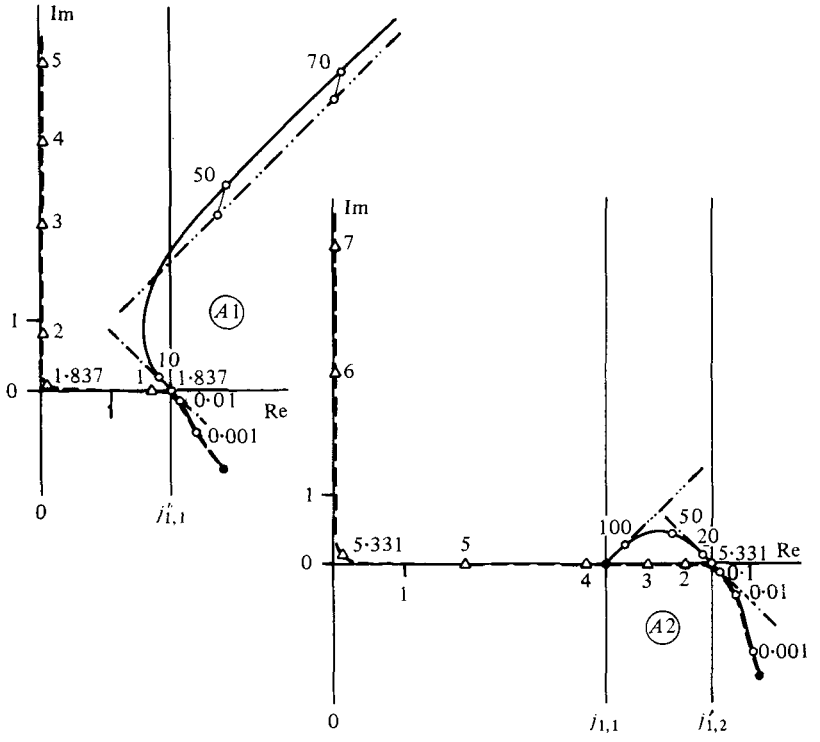

FIGURE 6. $M_{v,An}$ (—○—) and K_{An} (—△—) ($n = 1, 2$) for $m = 1$, $\gamma = 1$, $\alpha = \frac{4}{3}$ and $\Lambda = 10^{-4}$ with ω as parameter (● limiting solutions $\omega = 0$ and $\omega \to \infty$). Approximations: —·— (4·33); —·—·— (4·34); —···— (4·35).

$$M_{v,An} = j_{m,n-1}\left\{1+\frac{1}{\eta\epsilon}\left(1+\frac{\gamma-1}{\sigma^{\frac{1}{2}}}\right)^{-1}+\ldots\right\}, \quad n > 1$$

$$\text{for } \left|\frac{j_{m,n-1}}{\eta\epsilon}\right| \ll 1, \ |\epsilon| \ll 1 \quad \text{(very high frequency range).} \quad (4.35)$$

To illustrate the behaviour of $M_{v,An}(\omega)$ and the ranges of validity of the above approximations, a few computer calculations, for which a complex Newton procedure was used, are shown in figures 4 to 6. In all the plots the K_{An} are also included to show their typical resonance behaviour; it has to be noted that for $m = 0$ the basic mode $A1$ shows no resonance whereas for $m > 0$ all A-band modes have a distinct resonance at $\omega \simeq j'_{m,n}$. In figure 4 furthermore the wavenumber K_{A1} for $m = 0$ is compared to K_{BT} obtained by Bergh & Tijdeman (1965) with a simplified theory in which radial pressure gradients are neglected: as a result one finds that the theory of Bergh & Tijdeman yields good results only for $|\eta\epsilon| \ll 1$ (cf. the detailed discussion in TH) as for $|\eta\epsilon| \geqslant O(1)$ the effect of higher modes on the basic mode $A1$ ($m = 0$) can no longer be neglected.

Now the remaining limiting solutions of the eigenvalue equation (4.3) can be attributed to the *B-band* whereby a distinction of the cases $m = 0$ and $m > 0$ is advisable as for $m > 0$ a strong coupling between *D-* and *B-band* having the same natural wavenumber M_u must be expected.

For $m = 0$ a first solution $M_{u,B1} \equiv 0$ is readily found which is shown in the appendix

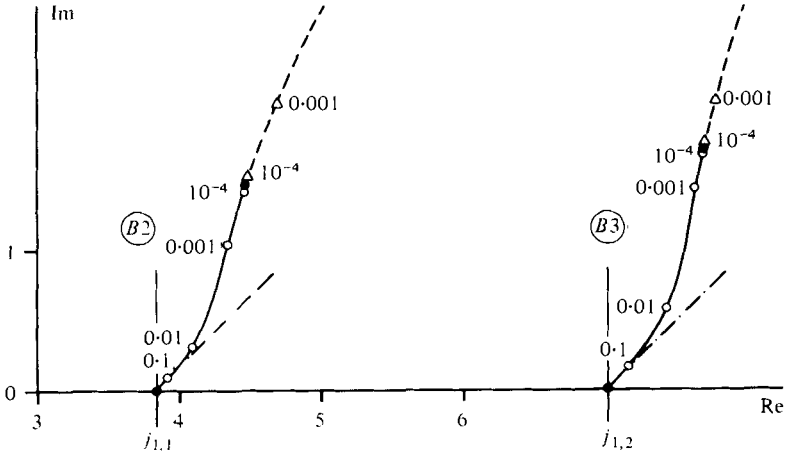

FIGURE 7. $M_{u,Bn}$ (—○—) and K_{Bn} (--△--) ($n = 2, 3$) for $m = 0$, $\gamma = 1{\cdot}4$, $\sigma = 0{\cdot}71$, $\alpha = \frac{4}{3}$ and $\Lambda = 10^{-4}$ with ω as parameter (● limiting solutions $\omega = 0$ and $\omega \to \infty$). Approximation (4.37), —·—.

to lead to the *trivial solution* of the problem. The solutions for $n > 1$ in the ultrahigh frequency range are then obtained as

$$M_{u,Bn} = j_{1,n-1}\left\{1+\frac{i}{\eta}\left(1-\frac{1}{\alpha}\right)^{\frac{1}{2}}+\ldots\right\}, \quad m = 0,\ n > 1$$

$$\text{for} \quad |\epsilon| \gg 1 \quad \text{(ultrahigh frequency range)}$$

$$\lim_{\omega\to\infty} M_{u,Bn} = j_{1,n-1}. \tag{4.36}$$

Analogously to the other bands also an approximation is obtained for the high to very high frequency range:

$$M_{u,Bn} = j_{1,n-1}\left\{1+\frac{i}{\eta}+O(\eta^{-2})\right\}, \quad m = 0,\ n > 1$$

$$\text{for} \quad |\epsilon| \ll 1, \left|\frac{j_{1,n-1}}{\eta}\right| \ll 1 \quad \text{(high and very high frequency range)}. \tag{4.37}$$

For $m > 0$ where $M_{u,Bn} = 0$ is no longer a solution of the eigenvalue equation (4.3) the corresponding approximations are obtained as:

$$M_{u,Bn} = j_{m-1,n}\left\{1+\frac{i}{2\eta}\left(1-\frac{1}{\alpha}\right)^{\frac{1}{2}}+\ldots\right\}, \quad m > 0 \quad \text{for} \quad |\epsilon| \gg 1$$

(ultrahigh frequency range)

$$\lim_{\omega\to\infty} M_{u,Bn} = j_{m-1,n}, \tag{4.38}$$

$$M_{u,Bn} = j_{m-1,n}\left\{1+\frac{i}{2\eta}+O(\eta^{-2})\right\}, \quad m > 0 \quad \text{for} \quad |\epsilon| \ll 1, \left|\frac{j_{m-1,n}}{\eta}\right| \ll 1$$

(high and very high frequency range). (4.39)

With figures 7 and 8 the typical behaviour of $M_{u,Bn}$ and K_{Bn} which show no resonance is illustrated for only one value of Λ as $M_{u,Bn}$ is almost entirely determined by the parameter η alone.

At this point all assertions of § 4.2 are proved and furthermore enough information on the actual values of the solutions of the general eigenvalue equation have been obtained to ensure a proper use of the eigensolutions, which are listed in the appendix.

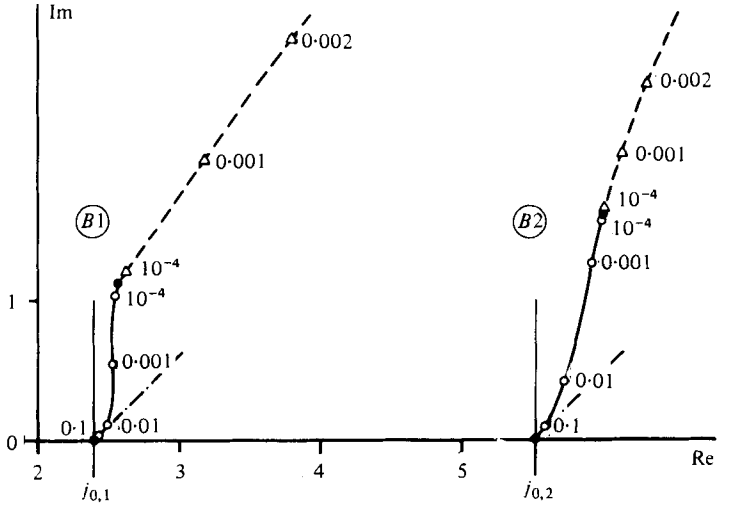

FIGURE 8. $M_{u,Bn}$ (—○—) and K_{Bn} (−−△−−) ($n = 1, 2$) for $m = 1, \gamma = 1, \alpha = \frac{4}{3}$ and $\Lambda = 10^{-4}$ with ω as parameter (● limiting solutions $\omega = 0$ and $\omega \to \infty$}. Approximation (4.39), —·—.

4.6. *The physical interpretation of the different bands*

In the literature the different bands of solutions are characterized by their dominant governing equations: the A-band modes governed mainly by (2.8) for ϕ are the pressure-dominated modes which is best recognized in the inviscid case (a) of § 4.2. Accordingly the C-band modes governed mainly by (2.9) for T are the temperature-dominated modes. Finally the B- and D-band modes governed mainly by (2.7) and (2.6) for ψ_θ and ψ_r respectively are then the vorticity-dominated modes. It has to be noted that this interpretation is consistent with the concept of the natural wavenumbers as they originate from the respective dominant equations.

In view of the use which will be made of the different eigenmodes to describe the total flow-field in the interior of a tube, the above characterization of modes is extended by specifying the spatial domain in which each mode can substantially contribute to the total field. The axial extension of this domain is thereby determined by the absolute magnitude of the damping Re[K]. Its radial extension on the other hand is evaluated by differentiating between 'core' terms and 'boundary-layer' terms: the terms in the eigensolutions (cf. appendix) depending on natural wavenumbers are clearly identified as core terms since the natural wavenumbers are always nearly real; all other terms which depend on wavenumbers with large imaginary part, contribute only to a 'boundary-layer' near $r = 1$ according to the following asymptotic estimates:

$$|M| \gg 1,\ |\arg[\mp iM]| < \tfrac{1}{2}\pi:$$

$$\left|\frac{J_m(Mr)}{J_m(M)}\right| \propto |(2\pi M)^{\frac{1}{2}} \exp[\pm iM]| \,.\, |J_m(Mr)| \ll 1 \quad \text{for} \quad |Mr| < 1,$$

$$\left|\frac{J_m(Mr)}{J_m(M)}\right| \propto \frac{1}{r^{\frac{1}{2}}} |\exp[\pm iM(1-r)]| = O(1) \quad \text{for} \quad |M(1-r)| \leqslant O(1). \tag{4.40}$$

Considering first the *A-band* it has to be noted that this is the only band in which |Re[K_{An}]| can be small. According to the discussion of the radial resonances in § 4.5, the damping of the mode An is small if the frequency ω is larger than its resonance

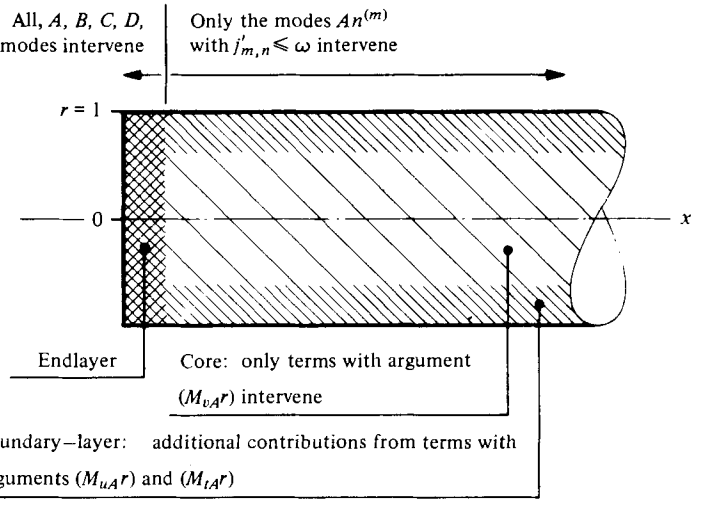

FIGURE 9. Domains of influence of the different modes.

frequency $\omega_{r,n} \simeq j'_{m,n}$ while the damping of the basic mode $A1(m = 0)$ is always small. So it is concluded that *all A-band modes with* $\omega \geqslant j'_{m,n}$ *contribute to the global flow-field* whereas *the modes An with* $\omega < j'_{m,n}$ *contribute only to the endlayers* at $x = 0$ and $x = L$.

In the *B-band* the damping $\mathrm{Re}[K_{Bn}] = \mathrm{Re}[(\eta^2 + M_{u,Bn})^{\frac{1}{2}}] \propto \mathrm{Re}[\eta]$ is already large at $\omega = 0$ (cf. table 2) and increases then monotonically with ω. As the 'reach' of the B-band modes is asymptotically given by the Stokes layer thickness $|\eta^{-1}|$, the B-band is characterized as the *Stokes endlayer-band.*

In the *C-band* the damping is given approximately by

$$\mathrm{Re}[K_{Cn}] \simeq \mathrm{Re}[(\eta^2\sigma + M^2_{t,Cn})^{\frac{1}{2}}] \propto \sigma^{\frac{1}{2}}\mathrm{Re}[\eta]$$

so that the above considerations for the B-band apply also to the C-band. Furthermore it is known from §§ 4.4 and 4.5 that $M_{t,Cn}$ is always very nearly equal to $j_{m,n}$ so that in the eigensolutions (cf. appendix) the temperature T and in the case $\gamma \neq 1$ also ρ largely dominate all other physical quantities. Thus the C-band is characterized as the *Stokes temperature and density endlayer-band.*

As both the *B-* and *D-band* have the same natural wavenumber M_u, all considerations for the B-band apply also to the D-band. A difference between these two bands is only found in the special case $m = 0$ where the D-band is a pure w-band (cf. § 4.2) so that it can be characterized as the *Stokes tangential endlayer-band.*

Summing up the results, the flow-field away from the endlayers is determined by a few low-order A-band modes, whereas all other modes intervene only near the tube ends to provide a proper transition between the imposed end-conditions and the 'inner' flow-field. This is shown schematically in figure 9 which might suggest an iterative procedure to satisfy the end-conditions, but it has to be pointed out immediately that this idea is in general not applicable as the 'inner' flow-field is a result of the balance of all modes at the ends.

5. The application of boundary conditions at the tube ends: the final solution

5.1. *The derivation of a general solution scheme*

At this point one has a set of eigenvectors (T, u, v, w), divided into bands, which are all solutions of the system of basic equations (2.6) to (2.9) and which fulfil the condition

(2.12) on the tube axis and the boundary conditions (2.13) at the tube perimeter. The aim of this section is to derive a general method to compute the amplitudes of these eigenvectors so that their sum fulfils the boundary conditions (2.15) at the tube ends.

The problem can be formulated using the concept of endvectors defined by (4.4). With the notation and normalization given in the appendix one has for every band an infinite set of axially growing (+) and damped (−) *eigen-endvectors* which will be denoted by $\mathscr{E}$:

$$\left.\begin{aligned}\mathscr{E}_n^+ &\equiv \begin{pmatrix} \hat{T}_n(r)\exp(-K_nL) \\ \hat{T}_n(r) \\ \hat{u}_n(r)\exp(-K_nL) \\ \hat{u}_n(r) \\ \hat{v}_n(r)\exp(-K_nL) \\ \hat{v}_n(r) \\ \hat{w}_n(r)\exp(-K_nL) \\ \hat{w}_n(r) \end{pmatrix}^{(m)} \exp(im\theta+i\omega t), \\ \mathscr{E}_n^- &\equiv \begin{pmatrix} -\hat{T}_n(r) \\ -\hat{T}_n(r)\exp(-K_nL) \\ \hat{u}_n(r) \\ \hat{u}_n(r)\exp(-K_nL) \\ -\hat{v}_n(r) \\ -\hat{v}_n(r)\exp(-K_nL) \\ -\hat{w}_n(r) \\ -\hat{w}_n(r)\exp(-K_nL) \end{pmatrix}^{(m)} \exp(im\theta+i\omega t).\end{aligned}\right\} \tag{5.1}$$

Omitting the factor $\exp(im\theta+i\omega t)$ in (5.1) and (2.15) one has the equation (5.2) to determine the unknown amplitudes C for every order (m):

$$\sum_{n=1}^{\infty}[C_{An}^+\mathscr{E}_{An}^+ + C_{An}^-\mathscr{E}_{An}^- + C_{Bn}^+\mathscr{E}_{Bn}^+ + C_{Bn}^-\mathscr{E}_{Bn}^- + C_{Cn}^+\mathscr{E}_{Cn}^+ + C_{Cn}^-\mathscr{E}_{Cn}^- + C_{Dn}^+\mathscr{E}_{Dn}^+ + C_{Dn}^-\mathscr{E}_{Dn}^-]^{(m)} = \begin{pmatrix} 0 \\ 0 \\ \hat{u}_e^{(m)}(r) \\ 0 \\ 0 \\ 0 \\ 0 \\ 0 \end{pmatrix} \equiv \mathscr{C}_e^{(m)}. \tag{5.2}$$

So far (5.2) is purely formal. The key to its practical solution is to consider the eigen-endvectors as elements of an appropriate Hilbert space, which is constructed in the following way: first it has to be noted that each of the 8 components of an endvector is itself an element of a Hilbert space $\mathbb{H}_q$ $(q = 1, \ldots, 8)$ containing the functions of r in the interval $[0, 1]$ with the scalar product and norm defined by

$$(f_q, g_q) = \int_0^1 f_q \bar{g}_q r\,dr; \quad \|f_q\|^2 = (f_q, f_q), \quad f_q, g_q \in \mathbb{H}_q. \tag{5.3}$$

By the following scalar product (5.4) the space $\mathbb{H}$ containing the endvectors (denoted by gothic characters) is defined as the direct sum of the component spaces $\mathbb{H}_q$.

$$\langle \mathscr{F}, \mathscr{G} \rangle = \sum_{q=1}^{8} \varphi_q(f_q, g_q) \tag{5.4}$$

$f_q, g_q \in \mathbb{H}_q$ being the components of $\mathscr{F}$, $\mathscr{G} \in \mathbb{H} = \bigoplus_{q=1}^{8} \mathbb{H}_q$ with the weighting factors φ_q satisfying the conditions

$$\varphi_q \text{real} > 0; \quad \sum_{q=1}^{8} \varphi_q = 1.$$

With the weighting factors a freedom has been built into the Hilbert space $\mathbb{H}$ which will be used for the adjustment of the relative convergence rates of the component series in (5.2), where convergence means always convergence in the norm.

For practical computations only a finite rather restricted number of eigen-endvectors can be retained so that the end-conditions (2.15) can only be approximated up to an error-endvector $\mathscr{D}^{(m)}$:

$$\left[\sum_{n=1}^{N_A^+} C_{An}^+ \mathscr{E}_{An}^+ + \sum_{n=1}^{N_A^-} C_{An}^- \mathscr{E}_{An}^- + \ldots + \sum_{n=1}^{N_D^-} C_{Dn}^- \mathscr{E}_{Dn}^-\right]^{(m)} + \mathscr{D}^{(m)}(N_A^+, N_A^-, N_B^+, N_B^-, N_C^+, N_C^-, N_D^+, N_D^-) = \mathscr{C}_e^{(m)}. \quad (5.5)$$

By the formulation of the problem in the appropriate space $\mathbb{H}$, the application of Galerkin's method (cf. Kantorovich & Krylov 1964) is now a straightforward matter. The Galerkin's equations (5.6) yield the best possible approximation to $\mathscr{C}_e^{(m)}$ in the sense that the norm $\langle \mathscr{D}^{(m)}, \mathscr{D}^{(m)} \rangle^{\frac{1}{2}}$ of the error-endvector in $\mathbb{H}$ is minimal for given $N_A^+ \ldots N_D^-$. In (5.6) the sum $N_A^+ + N_A^- + \ldots + N_D^-$ has been put equal to N and the band indices have been omitted.

$$\left[\sum_{n=1}^{N} C_n \langle \mathscr{E}_n, \mathscr{E}_k \rangle\right]^{(m)} = \langle \mathscr{C}_e, \mathscr{E}_k \rangle^{(m)}, \quad k = 1, \ldots, N. \quad (5.6)$$

With (5.6) the final solution for arbitrary end conditions – not only for the special choice (2.15) – is obtained and the problem with the simultaneous approximation of end conditions is generally solved without the need of additional considerations such as in the proposition made by Scarton (1970) which is shown in TH to be not generally valid. However three questions have been left open for discussion in the above analysis: first the suitable choice of the weighting factors φ_q in (5.4) which is preferably made *a priori*. Second the question arises whether there is an optimal choice for the individual numbers N_A^+ to N_D^- once the total number N is fixed. Third the completeness of the eigen-endvectors $\mathscr{E}$ in $\mathbb{H}$ has to be investigated.

5.2. *The determination of the weighting factors and the optimal number of eigen-endvectors from each band*

As the weighting factors appear as artificial parameters in the problem, the final exact solution has to be independent of them. This is in fact true if the completeness of the eigen-endvectors in $\mathbb{H}$ (cf. § 5.3) is assumed: the completeness involves the vanishing of $\langle \mathscr{D}^{(m)}, \mathscr{D}^{(m)} \rangle$ in (5.5) as $N_A^+ \ldots N_D^-$ tend to infinity. From the definition (5.4) it is then obvious that all component norms of $\mathscr{D}^{(m)}$ vanish separately irrespective of the φ's. Thus the weighting factors can be used freely to influence the relative magnitude of the components of $\mathscr{D}^{(m)}$ and could be determined iteratively by Lawson's algorithm (cf. Ellacott & Williams 1976) to yield any desired ratio of the component norms of $\mathscr{D}^{(m)}$. This procedure is nevertheless not adopted because of its complication and because the free choice of the φ's is severely constrained by the limited accuracy in numerical

calculations: for good results it is required that at most in the important scalar products $\langle\ \rangle$ all component scalar products are of the same order of magnitude.

Considering the expressions (5.1) for the eigen-endvectors a first choice is made by setting $\varphi_1 = \varphi_2 \equiv \varphi_T$, $\varphi_3 = \varphi_4 \equiv \varphi_u$, $\varphi_5 = \varphi_6 \equiv \varphi_v$, $\varphi_7 = \varphi_8 \equiv \varphi_w$, thus defining only 4 weighting factors associated with the physical quantities. To make the most important component scalar products the same order of magnitude, three cases have to be considered:

Away from radial resonances the above requirement is matched by the following ratio:

$$(\varphi_T{:}\varphi_u{:}\varphi_v{:}\varphi_w) = (1{:}1{:}1{:}1). \tag{5.7}$$

At a *radial resonance with* $L = \infty$ clearly the resonant eigenvector An is dominant. Using the expansions (4.16) and (4.33) $|K_{An}|$ is found to be of the order $\Lambda^{\frac{1}{4}}$. As $\|\hat{T}_{An}\|^2$, $\|\hat{v}_{An}\|^2$, $\|\hat{w}_{An}\|^2$ are of order $|K_{An}|^{-2}$ (cf. appendix) whereas $\|\hat{u}_{An}\|^2$ is of order unity, the appropriate ratio in this case is

$$(\varphi_T{:}\varphi_u{:}\varphi_v{:}\varphi_w) = (1{:}\Lambda^{-\frac{1}{2}}{:}1{:}1). \tag{5.8}$$

At a *radial resonance with finite* L additional difficulties occur when the conditions on u at both ends have to be satisfied by weakly damped eigensolutions with a long wavelength compared to L. By considering the combination $\mathscr{E}^-_{An} - \exp(-K_{An}L)\,\mathscr{E}^+_{An}$ of the resonant eigen-endvectors in which $u(x = L) = 0$, the difficulty is traced back to the factor $[1 - \exp(-2K_{An}L)]$ being small, $O(L\Lambda^{\frac{1}{4}})$. This suggests the modification of the ratio (5.8) to

$$(\varphi_T{:}\varphi_u{:}\varphi_v{:}\varphi_w) = (1{:}L^{-1}\Lambda^{-\frac{3}{4}}{:}1{:}1). \tag{5.9}$$

To optimize the ratio of the numbers $N^+_A \ldots N^-_D$ for a given total number of eigen-endvectors N one has to realize that the error is composed of two parts: a basic part which arises from the number N being finite and a second part which is determined by the amount of interference between concurrent end conditions. The way to minimize this interference or 'compromise' error is found by an argument on the possibility of constructing pure endvectors introduced in § 4.2 out of a finite number of $\mathscr{E}$'s. To eliminate for instance the first component in all the N^+_A eigen-endvectors $\mathscr{E}^+_{An}$ by appropriately combining each of the $\mathscr{E}^+_{An}$ with say the N^-_C eigen-endvectors $\mathscr{E}^-_{Cn}$, the linear span of the N^+_A functions $\hat{T}_{An}$ must be identical to the linear span of the N^-_C functions $\hat{T}_{Cn}$. Carrying this argument through all the bands and components one finds that for each component the component-functions of every band must have the same linear span. Under this condition eight bands of pure endvectors can be constructed and all end conditions can be matched independently in an optimal way without additional interference errors. It is therefore concluded that the condition of equality of linear spans has to be matched as precisely as possible. Considering the results of § 4 this is achieved by setting

$$\text{for}\quad m = 0\colon\ N_B = N_C = N_A - 1;\ N_D \text{ arbitrary},$$

$$\text{for}\quad m > 0\colon N_B = N_C = N_D = N_A,$$

with

$$N^+_A = N^-_A \equiv N_A,\quad N^+_B = N^-_B \equiv N_B,\quad N^+_C = N^-_C \equiv N_C,\quad N^+_D = N^-_D \equiv N_D. \tag{5.10}$$

The choice for $m = 0$ is thereby motivated by the special role of the mode $A1$ which has no counterpart in the B-band and by the D-band being decoupled.

Finally it has to be assured that $\hat{u}_e^{(m)}(r)$ in (2.15) can be reasonably approximated which means that a major portion of $\hat{u}_e^{(m)}$ has to be contained in the linear span of say the N_A functions $\hat{u}_{An}^{(m)}$.

5.3. *The completeness of the eigen-endvectors in* $\mathbb{H}$

The most difficult question in connexion with the matching of end-conditions is whether the eigen-endvectors $\mathscr{E}$ which are divided into eight bands form a complete set of elements of $\mathbb{H}$, where completeness means the vanishing of the error $\mathscr{D}^{(m)}$ in (5.5) for *arbitrary* $\mathscr{C}_e^{(m)} \in \mathbb{H}$ as $N_A, N_B, N_C, N_D \to \infty$.

A rigorous proof has not been attempted, but a numerical check has been performed in the axisymmetric case $m = 0$ with a computer program consisting of several parts: in a first step the approximate eigenvalues of § 4 are improved by a complex Newton procedure using the idea of natural wavenumbers. Thereby the Bessel functions are calculated with utmost care to an accuracy of 13–14 digits (*CDC* single precision) using their series expansion, Hankel's asymptotic expansion and expansions around their zeroes (Detournay & Piessens 1971). Second the scalar products $\langle\ \rangle$ in the Galerkin's equations are calculated by evaluating analytically all the component scalar products (5.3). Third the system of Galerkin's equations (5.6) is solved by the method of Cholesky's triangle decomposition (Schwarz, Rutishauser & Stiefel 1972) and lastly the total norm of the error $\mathscr{D}^{(0)}$ is calculated together with its component norms. With this program four different combinations of Λ and ω with two end-conditions (2.15) denoted by (*PL*) and (*PI*) and defined below have been investigated.

(*PL*) excitation by an oscillating plate at $x = 0$

$$\hat{u}_e^{(0)} = 1 - \frac{J_0(j_{1,1} r)}{J_0(j_{1,1})}, \tag{5.11}$$

(*PI*) excitation by a plane piston at $x = 0$

$$\hat{u}_e^{(0)} = 2^{\frac{1}{2}}. \tag{5.12}$$

Except for the case (*PI*) at high frequency which is questionable because of nonlinear effects (cf. § 2) and where also the number of modes was insufficient, all calculations showed in the range $N_A \in [3, 21]$ a convergence to zero of every single component norm of the error $\mathscr{D}^{(0)}$ at least like $N_A^{-\frac{1}{2}}$. This gives a sound indication that the procedure converges at least like the convergent series Σn^{-2} and that the $\mathscr{E}$'s are complete in $\mathbb{H}$. Furthermore the $\mathscr{E}$'s are found to be also linearly independent. Finally the pointwise convergence is established by the fact that the amplitudes of the most important modes converge towards limits which are reasonably independent of the weighting factors (cf. TH for detailed results).

6. Examples of radial resonance and end-layers

6.1. *Analytic results for the radial resonance case with rotational symmetry and* $\gamma \neq 1$

A first discussion of the radial resonance case in § 4.5 has shown that the behaviour of the radial velocity is essentially determined by the factor $M_{v,An}/K_{An}$ (cf. the expression A 2 for $\hat{v}$ in the appendix). In fact it has been shown that $|K_{An}|$ has a sharp minimum for $\omega \simeq j'_{0,n}$ and $n \geqslant 2$ whereas $M_{v,An}$ remains nearly constant around this frequency. Thus

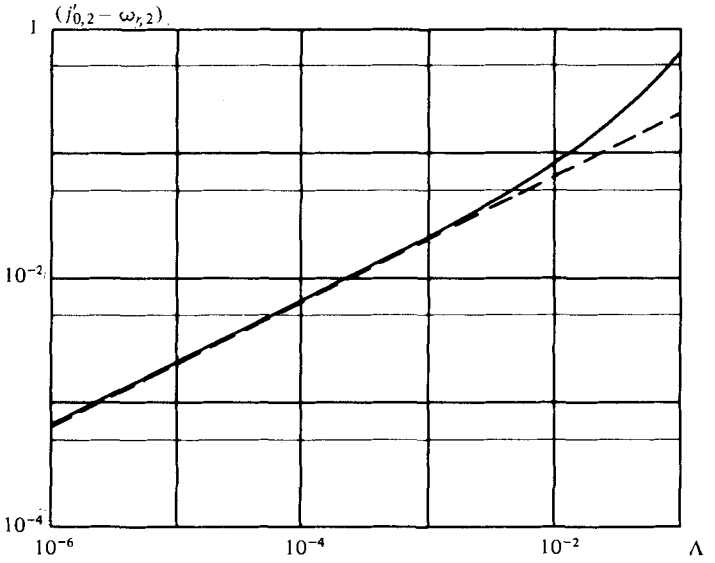

FIGURE 10. Departure of the resonance frequency $\omega_{r,2}$ of the mode $A2$ from its inviscid value $j'_{0,2}$ versus Λ for air ($m = 0, \gamma = 1{\cdot}4, \sigma = 0{\cdot}71, \alpha = \frac{4}{3}$): numerical calculation, ——; and approximation (6.2), – – –.

it is obvious to define the *resonance frequency* $\omega_{r,n}$ of the nth A-band mode as the frequency at which the factor $|M_{v,An}/K_{An}|$ has its maximum value – or in other words at which $\|\hat{v}_{An}\|$ attains its peak value with a given excitation of $\hat{u}_{An}$. Using the high frequency approximation (4.33) for $M_{v,An}$ and the expansion (4.16) to calculate K_{An}, one finds upon replacing ϵ and η by their definitions:

$$\left.\begin{aligned} M^2_{v,An} &= j'^2_{0,n} - 2i^{\frac{3}{2}}\Lambda^{\frac{1}{2}}\frac{j'^2_{0,n}}{\omega^{\frac{1}{2}}}\left[1 - \frac{\omega^2 S}{j'^2_{0,n}}\right] + O(\Lambda), \\ \text{with} \qquad S &= 1 + \frac{\gamma - 1}{\sigma^{\frac{1}{2}}}, \\ K^2_{An} &= [j'^2_{0,n} - \omega^2] - 2i^{\frac{3}{2}}\Lambda^{\frac{1}{2}}\frac{j'^2_{0,n}}{\omega^{\frac{1}{2}}}\left[1 - \frac{\omega^2 S}{j'^2_{0,n}}\right] + O(\Lambda) \\ \text{for} \quad m = 0 \quad &\text{(rotational symmetry)} \quad \text{and} \quad \gamma \neq 1. \end{aligned}\right\} \tag{6.1}$$

With these expressions the maximum of $|M_{v\,An}/K_{An}|$ is found at:

$$\omega_{r,n} = j'_{0,n}\left\{1 - (\gamma - 1)\left(\frac{\Lambda}{2\sigma j'_{0,n}}\right)^{\frac{1}{2}} + O(\Lambda)\right\}, \tag{6.2}$$

with $$\left|\frac{M_{v,An}}{K_{An}}\right|(\omega_{r,n}) = \left\{\frac{2\Lambda(\gamma-1)^2}{\sigma j'_{0,n}}\right\}^{-\frac{1}{4}} + \ldots, \quad \text{for} \quad m = 0 \quad \text{and} \quad \gamma \neq 1. \tag{6.3}$$

In figure 10 the approximation (6.2) for the resonance frequency $\omega_{r,2}$ of the mode $A2$ is compared to numerical calculations for different Λ whereby the correspondence is found to degrade above $\Lambda = 10^{-3}$.

Besides the good approximation (6.2) for the resonance frequency, information on the *shape of the resonance curve*, i.e. on the behaviour of $\|C_{An}\hat{v}_{An}\|$ in the neighbourhood of $\omega_{r,n}$, is also desirable. The problem which occurs here is the determination of the amplitude C_{An}: in general C_{An} can only be obtained by going through the whole pro-

cedure described in § 5 and depends naturally on the end-conditions. But as by numerical evidence the amplitude C_{An} is nearly constant in a neighbourhood of $\omega_{r,n}$, this difficulty is circumvented by normalizing $\|C_{An}\hat{v}_{An}\|$ with its value at the resonance. Setting $\omega = \omega_{r,n} + \Delta\omega$ and using the approximations (6.2) and (6.3) one finds:

$$\frac{\|C_{An}\hat{v}_{An}\|}{\|C_{An}\hat{v}_{An}\|_r} \simeq \frac{\|\hat{v}_{An}\|}{\|\hat{v}_{An}\|_r} \simeq \left|\frac{M_{v,An}}{K_{An}}\right|(\omega).\left|\frac{M_{v,An}}{K_{An}}\right|^{-1}(\omega_{r,n})$$

$$\simeq \left\{1+\frac{2\sigma}{\Lambda(\gamma-1)^2 j'_{0,n}}\,\Delta\omega^2\left[1+\frac{\Delta\omega}{j'_{0,n}}\right]\right\}^{-\frac{1}{4}}, \qquad (6.4)$$

with $\omega = \omega_{r,n} + \Delta\omega$ and $\omega_{r,n}$ given by (6.2) $(m = 0,\ \gamma \neq 1)$.

This approximation (6.4) which is compared to numerical calculations in § 6.2, is of some importance as it is possible to determine approximately the reference quantity $\|C_{A2}\hat{v}_{A2}\|_r$ in the case where the oscillation in a half-infinite tube ($L = \infty$) is excited by the end-condition (PL) defined by (5.11). To this the general method of § 5 is applied with the following simplifications: when dealing with a half-infinite tube, only the axially damped eigen-endvectors $\mathscr{E}^-$ (cf. 5.1) have to be considered in which, furthermore, only the components $T(x=0)$, $u(x=0)$ and $v(x=0)$ have to be retained, as for $m = 0$, w is identically zero. Then the component $T(x=0)$ can be omitted as it is possible with the nearly pure $\mathscr{E}^-_{Cn}$ to satisfy *a posteriori* the end-condition for T, while leaving the results for u and v unchanged up to higher-order corrections. Finally the success of the approximation justifies the restriction to the absolutely necessary eigen-endvectors $\mathscr{E}^-_{A1}$, $\mathscr{E}^-_{A2}$ and $\mathscr{E}^-_{B2}$.

To determine the scalar products involved in the Galerkin's equations (5.6) around the resonance frequency $\omega_{r,2}$ of the mode $A2$ ω may be written as

$$\omega = \omega_{r,2} + c\Lambda^{\frac{1}{2}} = j + \Lambda^{\frac{1}{2}}\left[c-(\gamma-1)\left(\frac{j}{2\sigma}\right)^{\frac{1}{2}}\right] + O(\Lambda), \qquad (6.5)$$

with $j \equiv j'_{0,2} = j_{1,1}$.

Introducing this expression into the high frequency approximations of § 4.5 and using the expansions (4.16) one finds for the $A1$, $A2$ and $B2$ wavenumbers:

$$\left.\begin{aligned}
M^2_{v,A1} &= 2i^{\frac{3}{2}}\Lambda^{\frac{1}{2}}Sj^{\frac{3}{2}} + O(\Lambda) \quad \text{with} \quad S = 1+\frac{\gamma-1}{\sigma^{\frac{1}{2}}},\\
K_{A1} &= ij + O(\Lambda^{\frac{1}{2}}),\\
M_{u,A1} &= -i^{\frac{3}{2}}(j/\Lambda)^{\frac{1}{2}} + O(1),\\
M_{t,A1} &= M_{u,A1}O^{\frac{1}{2}} + O(1),\\
M_{v,A2} &= j + i^{\frac{3}{2}}(\Lambda j)^{\frac{1}{2}}\frac{\gamma-1}{\sigma^{\frac{1}{2}}} + O(\Lambda),\\
K_{A2} &= i^{\frac{1}{2}}\Lambda^{\frac{1}{2}}(2j)^{\frac{1}{2}}Q \quad \text{with} \quad Q = \left[(\tfrac{1}{2}j)^{\frac{1}{2}}\frac{\gamma-1}{\sigma^{\frac{1}{2}}} + ic\right]^{\frac{1}{2}},\\
M_{u,A2} &= M_{u,A1} + O(1),\\
M_{t,A2} &= M_{t,A1} + O(1),\\
M_{u,B2} &= j + i^{\frac{1}{2}}(\Lambda j)^{\frac{1}{2}} + O(\Lambda),\\
K_{B2} &\simeq M_{v,B2} = i^{\frac{1}{2}}(j/\Lambda)^{\frac{1}{2}} + O(1),\\
M_{t,B2} &= K_{B2}.(1-\sigma)^{\frac{1}{2}} + O(1).
\end{aligned}\right\} \qquad (6.6)$$

Evaluating the integrals (5.3) and expanding the Bessel functions, the component norms and scalar products of the eigen-endvectors involved are obtained. Discarding all quantities of higher order in Λ one finds:

$$\left.\begin{aligned}
&\|\hat{u}_{A1}\|^2 = 1+O(\Lambda^{\frac{1}{2}}) \quad \|\hat{v}_{A1}\|^2 = O(\Lambda),\\
&\|\hat{T}_{A1}\|^2 = 1+O(\Lambda^{\frac{1}{2}}),\\
&\|\hat{u}_{A2}\|^2 = 1+O(\Lambda^{\frac{1}{2}}), \quad \|\hat{v}_{A2}\|^2 = \frac{j}{2\Lambda^{\frac{1}{2}}Q\bar{Q}}+O(1),\\
&\|\hat{T}_{A2}\|^2 = \|\hat{v}_{A2}\|^2+O(1),\\
&\|\hat{u}_{B2}\|^2 = 1+O(\Lambda^{\frac{1}{2}}), \quad \|\hat{v}_{B2}\|^2 = \frac{1}{\Lambda j}+O\left(\frac{1}{\Lambda^{\frac{1}{2}}}\right),\\
&\|\hat{T}_{B2}\|^2 = O(\Lambda^{\frac{1}{2}}),\\
&(\hat{v}_{A2}, \hat{v}_{B2}) = \frac{i}{2^{\frac{1}{2}}\Lambda^{\frac{3}{4}}Q}+O(\Lambda^{-\frac{1}{4}}),\\
&(\hat{u}_{A2}, \hat{u}_{B2}) = -1+O(\Lambda^{\frac{1}{2}}),\\
&(\hat{u}_e^{(0)}, \hat{u}_{A1}) = \frac{1}{2^{\frac{1}{2}}}+O(\Lambda^{\frac{1}{2}}),\\
&(\hat{u}_e^{(0)}, \hat{u}_{A2}) = -\frac{1}{2^{\frac{1}{2}}}+O(\Lambda^{\frac{1}{2}}),\\
&(\hat{u}_e^{(0)}, \hat{u}_{B2}) = \frac{1}{2^{\frac{1}{2}}}+O(\Lambda^{\frac{1}{2}}) \quad \text{with} \quad \hat{u}_e^{(0)} = 1-\frac{J_0(jr)}{J_0(j)} \ (PL).
\end{aligned}\right\} \tag{6.7}$$

Combining the above component scalar products with the weighting factors (5.8) to the scalar products $\langle\ \rangle$, the Galerkin equations (5.6) take the following form:

$$\left.\begin{aligned}
&C_{A1}^{-}\frac{1}{\Lambda^{\frac{1}{2}}} = \frac{1}{(2\Lambda)^{\frac{1}{2}}},\\
&C_{A2}^{-}\frac{1}{\Lambda^{\frac{1}{2}}}\left[1+\frac{j}{2Q\bar{Q}}\right]-C_{B2}^{-}\frac{1}{\Lambda^{\frac{1}{2}}}\left[\frac{i}{\Lambda^{\frac{1}{4}}2^{\frac{1}{2}}\bar{Q}}+1\right] = -\frac{1}{(2\Lambda)^{\frac{1}{2}}},\\
&C_{A2}^{-}\frac{1}{\Lambda^{\frac{1}{2}}}\left[\frac{i}{\Lambda^{\frac{1}{4}}2^{\frac{1}{2}}Q}-1\right]+C_{B2}^{-}\frac{1}{\Lambda j} = \frac{1}{(2\Lambda)^{\frac{1}{2}}},
\end{aligned}\right\} \tag{6.8}$$

with the solutions:

$$\left.\begin{aligned}
&C_{A1}^{-} = \frac{1}{2^{\frac{1}{2}}}+O(\Lambda^{\frac{1}{2}}),\\
&C_{A2}^{-} = -\frac{1}{2^{\frac{1}{2}}}+\Lambda^{\frac{1}{4}}\frac{ij_{1,1}}{2}\left[\left(\frac{j_{1,1}}{2}\right)^{\frac{1}{2}}\frac{(\gamma-1)}{\sigma^{\frac{1}{2}}}+ic\right]^{-\frac{1}{2}}+O(\Lambda^{\frac{1}{2}}),\\
&C_{B2}^{-} = -\Lambda^{\frac{1}{4}}\frac{ij_{1,1}}{2^{\frac{1}{2}}}\left[\left(\frac{j_{1,1}}{2}\right)^{\frac{1}{2}}\frac{(\gamma-1)}{\sigma^{\frac{1}{2}}}+ic\right]^{-\frac{1}{2}}C_{A2}^{-}+O(\Lambda^{\frac{3}{4}}),\\
&\text{with} \quad \omega = j_{1,1}+\Lambda^{\frac{1}{2}}\left[c-(\gamma-1)\left(\frac{j_{1,1}}{2\sigma}\right)^{\frac{1}{2}}\right],\\
&\text{for} \quad m = 0,\ L = \infty,\ \gamma \neq 1,\ \omega = \omega_{r,2}+c\Lambda^{\frac{1}{2}} \quad \text{and the excitation } (PL)\\
&\text{defined by (5.11).}
\end{aligned}\right\} \tag{6.9}$$

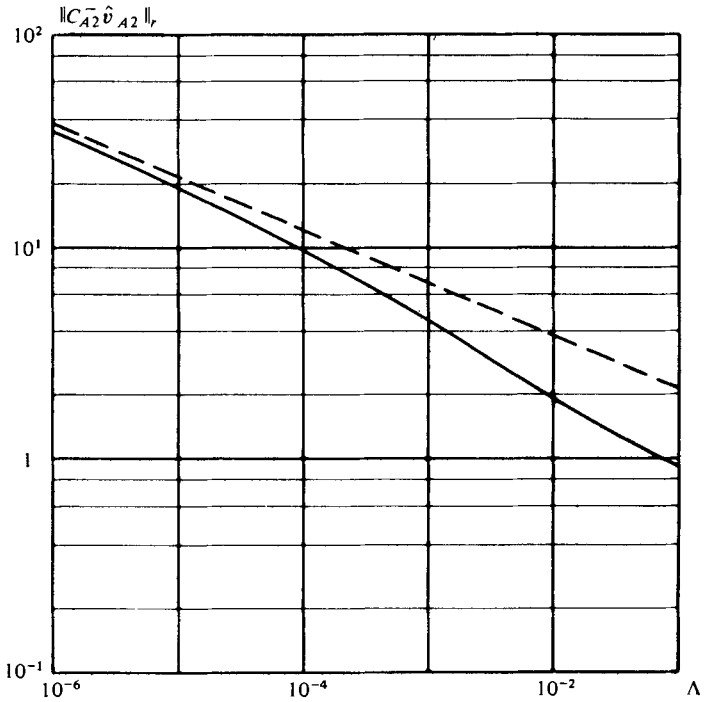

FIGURE 11. Norm of the maximal radial velocity in the resonance of the mode $A2$ versus Λ: numerical calculation, ——; approximation (6.10), – – –. Parameters: $m = 0$, $L = \infty$, $N_A = 16$, excitation (PL); $\gamma = 1{\cdot}4$, $\sigma = 0{\cdot}71$, $\alpha = \frac{4}{3}$.

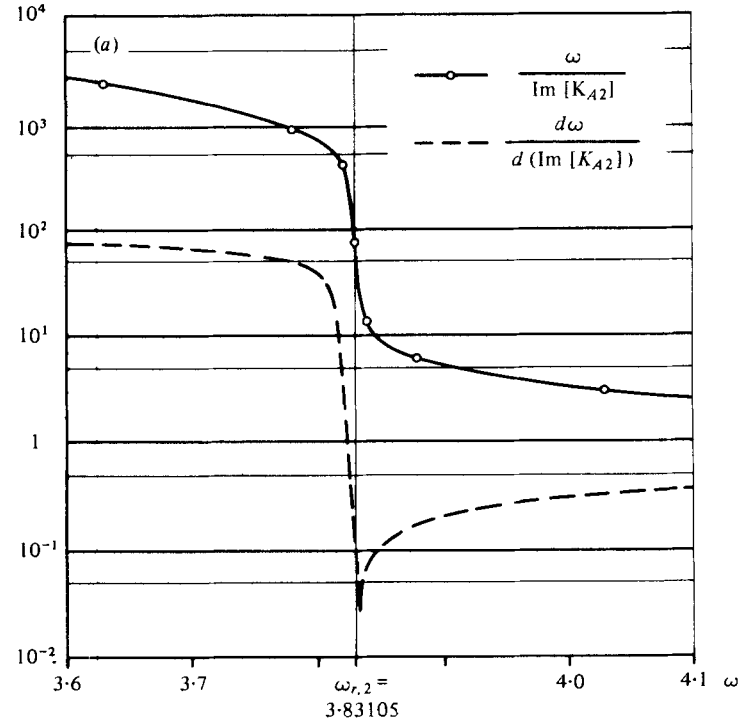

FIGURE 12 (*a*). For legend see page 387.

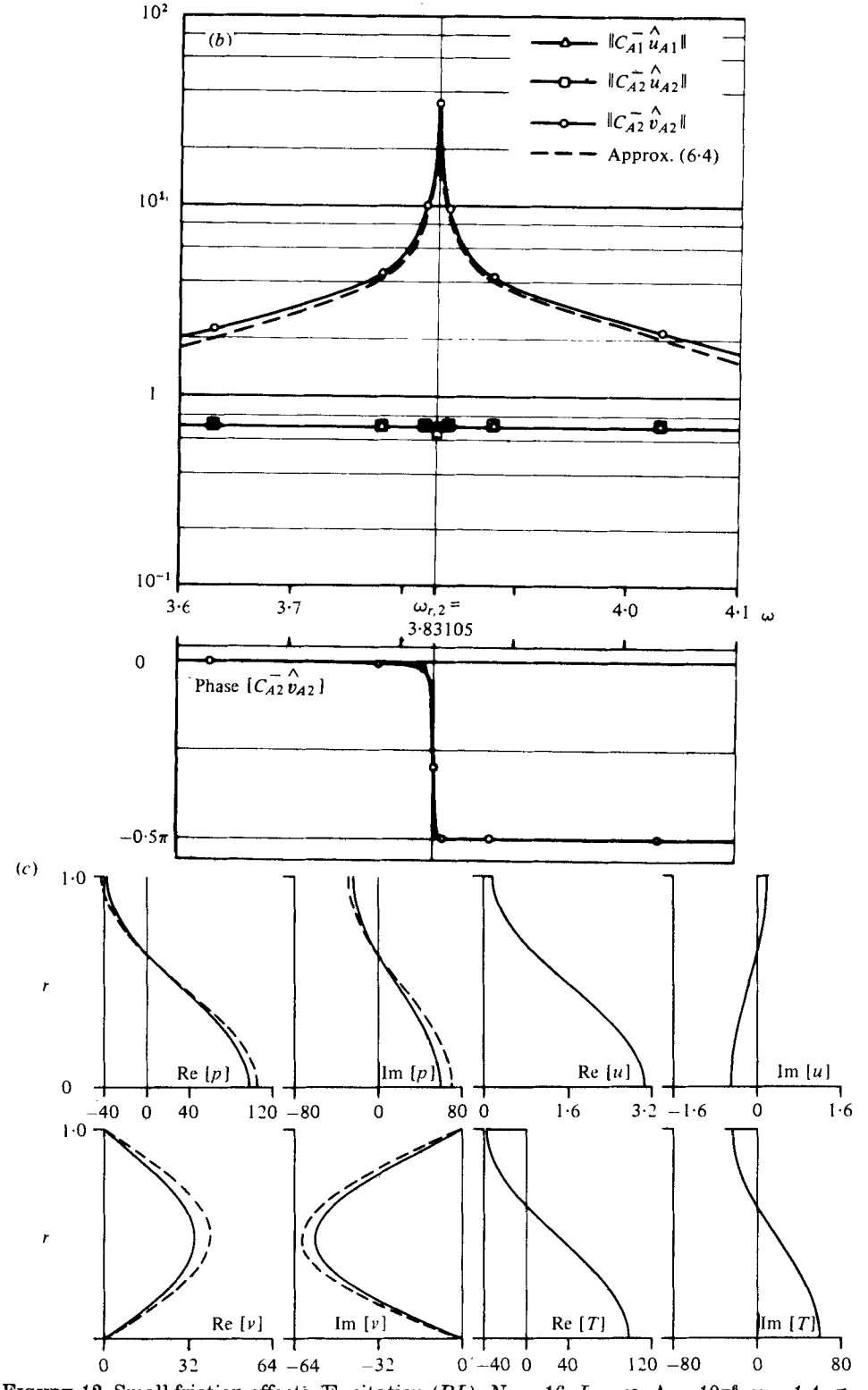

FIGURE 12. Small friction effects. Excitation (PL), $N_A = 16$, $L = \infty$, $\Lambda = 10^{-6}$, $\gamma = 1{\cdot}4$, $\sigma = 0{\cdot}71$, $\alpha = \frac{4}{3}$. (*a*) Phase and group velocity versus ω; (*b*) Resonance curve and phase versus ω; (*c*) Flow-field at the resonance of the mode $A2$ ($\omega_{r,2} = 3{\cdot}83105$) at $x = 1{\cdot}63920$: numerical calculation, ——; approximation (6.11), – – –.

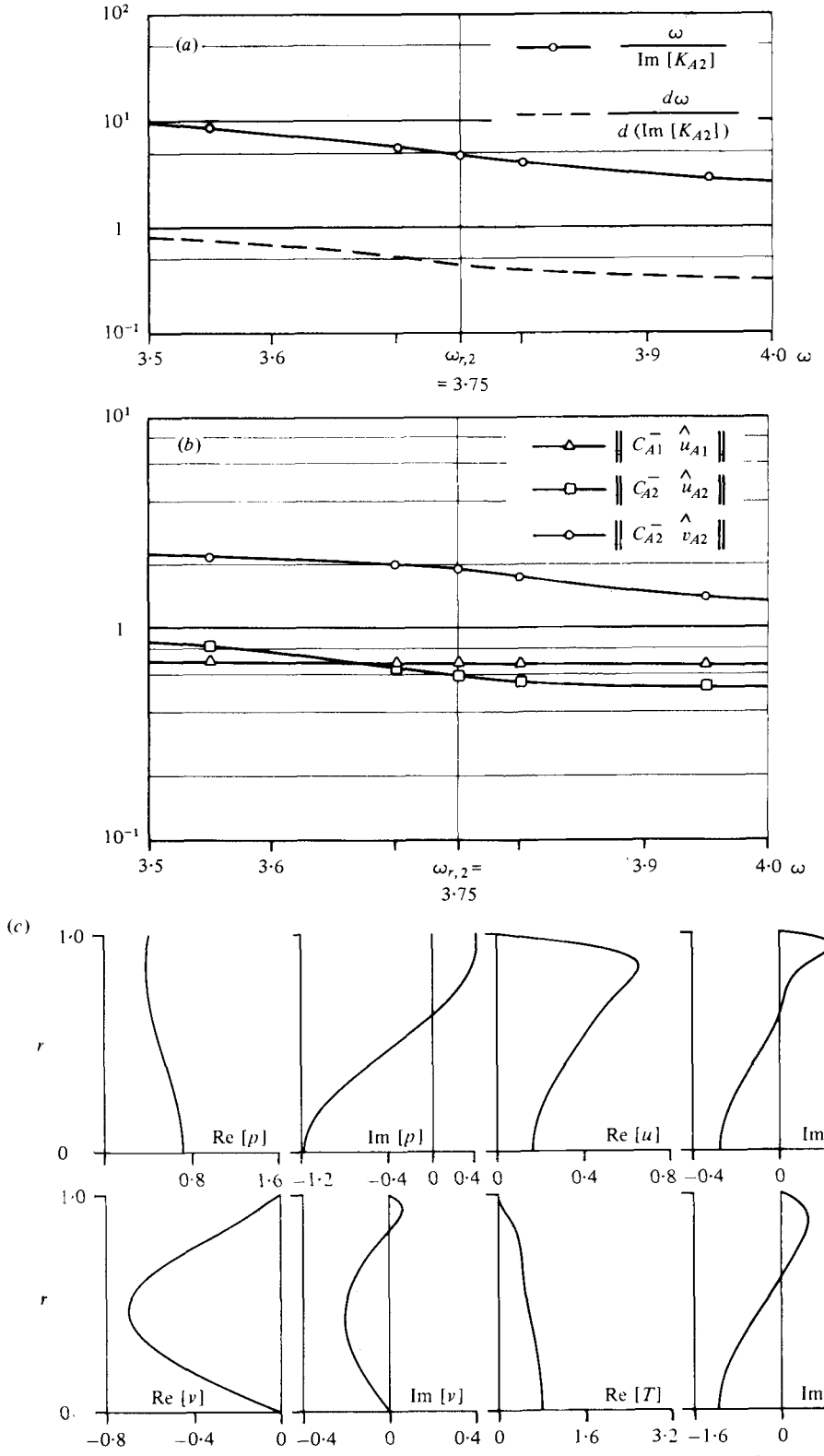

FIGURE 13. Large friction effects. Excitation (PL), $N_A = 16$, $L = \infty$, $\Lambda = 10^{-2}$, $\gamma = 1{\cdot}4$, $\sigma = 0{\cdot}71$, $\alpha = \frac{4}{3}$. (*a*) Phase and group velocity versus ω; (*b*) 'Resonance curve' versus ω; (*c*) Flow-field at the 'resonance' of the mode $A2$ ($\omega_{r,2} = 3{\cdot}75$) at $x = 1{\cdot}605$.

So the reference quantity $\|C^-_{An}\hat{v}_{An}\|_r$ in (6.4) can indeed be determined approximately for this particular case:

$$\|C^-_{A2}\hat{v}_{A2}\|_r \cong \frac{(j_{1,1})^{\frac{1}{2}}}{2\Lambda^{\frac{1}{4}}}\left[\frac{j_{1,1}(\gamma-1)^2}{2\sigma}\right]^{-\frac{1}{4}}, \tag{6.10}$$

for $m = 0$, $L = \infty$, $\gamma \neq 1$, $\omega = \omega_{r,2}$ and the excitation (PL).

In figure 11 this result shows good agreement not only in the exponent of Λ but also in absolute magnitude with numerical calculations for $\Lambda < 10^{-4}$. The result (6.9) not only allows the determination of resonance curves, but can also be used to compute directly the physical quantities p and v which are of particular interest in a radial resonance. Upon expanding the exponential factors $\exp(-Kx)$ one finds outside the endlayer of thickness $O(|\eta|^{-1})$ where the mode $B2$ is damped out the following expressions, which are compared to numerical results in § 6.2:

$$\left.\begin{aligned} p &= p^-_{A1} + p^-_{A2}, \\ p^-_{A1} &= 1 + O(\Lambda^{\frac{1}{2}}), \\ p^-_{A2} &= -i^{\frac{1}{2}}\frac{(j_{1,1})^{\frac{1}{2}}}{\Lambda^{\frac{1}{4}}2^{\frac{1}{2}}Q}\left\{1-\Lambda^{\frac{1}{4}}\left[i\frac{j_{1,1}}{2^{\frac{1}{2}}Q}+i^{\frac{1}{2}}(2j_{1,1})^{\frac{1}{2}}Qx\right]\right\}\frac{J_0(j_{1,1}r)}{J_0(j_{1,1})}, \\ v = v^-_{A2} &= i^{\frac{3}{2}}\frac{(j_{1,1})^{\frac{1}{2}}}{\Lambda^{\frac{1}{4}}2^{\frac{1}{2}}Q}\left\{1-\Lambda^{\frac{1}{4}}\left[i\frac{j_{1,1}}{2^{\frac{1}{2}}Q}+i^{\frac{1}{2}}(2j_{1,1})^{\frac{1}{2}}Qx\right]\right\}\frac{J_1(j_{1,1}r)}{J_0(j_{1,1})}, \\ \text{with} \qquad Q &= \left[\frac{j_{1,1}(\gamma-1)^2}{2\sigma}\right]^{\frac{1}{4}}, \\ \text{for} \qquad & m = 0,\ L = \infty,\ \gamma \neq 1,\ \omega = \omega_{r,2} \text{ and the excitation } (PL). \end{aligned}\right\} \tag{6.11}$$

6.2. *Computer calculations for radial resonance cases with rotational symmetry*

In this section two examples of the radial resonance of the mode $A2(m = 0)$ in a half-infinite tube – one with small and one with large friction effects – are shown. Because of the difficulties occurring with a plane piston which were discussed in conjunction with the boundary conditions, the excitation with the oscillating plate (PL) defined by (5.11) has been chosen.

In both cases the phase and group velocity of the mode $A2$ is plotted. Thereby it has to be noted that the usual concept of group velocity, defined by $d\omega/d(\mathrm{Im}\,[K])$, becomes meaningless for large damping $\mathrm{Re}\,[K] \geqslant O(\mathrm{Im}\,[K])$. For comparison the phase and group velocities in the inviscid case (c.f. § 4.2) are given by:

$$\left.\begin{aligned} &\text{Phase velocity} \quad u_{Ph} = \omega/\mathrm{Im}\,[K_{A2}], \\ &u_{Ph} = \infty, \qquad \omega \leqslant j_{1,1}(= 3{\cdot}83171), \\ &u_{Ph} = \omega/(\omega^2 - j^2_{1,1})^{\frac{1}{2}} \quad \omega > j_{1,1}. \end{aligned}\right\} \tag{6.12}$$

$$\left.\begin{aligned} &\text{Group velocity} \quad u_{Gr} = d\omega/d(\mathrm{Im}\,[K_{A2}]), \\ &u_{Gr} = \infty, \qquad \omega \leqslant j_{1,1}, \\ &u_{Gr} = (\omega^2 - j^2_{1,1})^{\frac{1}{2}}/\omega, \quad \omega > j_{1,1}. \end{aligned}\right\} \tag{6.13}$$

Thus a transition of the mode $A2$ occurs in the resonance from a strongly damped standing wave to a running wave which is undamped in the inviscid case. The effect

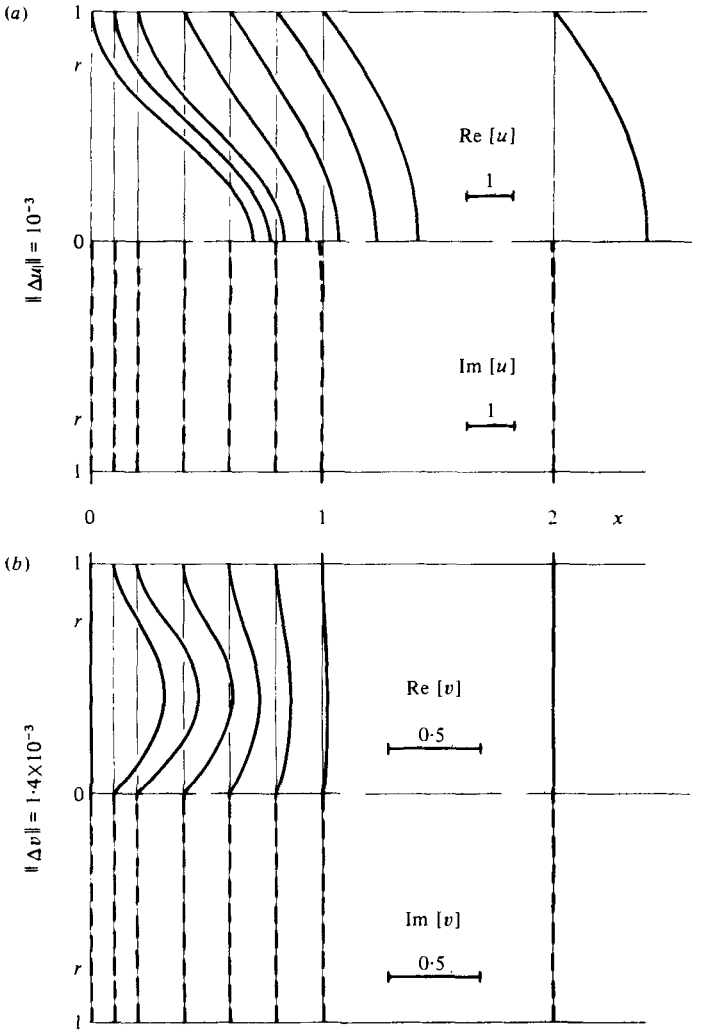

FIGURE 14 (*a*, *b*). For legend see page 391.

of viscosity on this behaviour is apparent in figures 12(*a*) and 13(*a*). The respective resonance curves are plotted in figures 12(*b*) and 13(*b*). In the case of small friction effects also the phase of $C_{A2}^{-}\hat{v}_{A2}$ is incorporated, as then it is constant over the whole core section. In figures 12(*c*) and 13(*c*) the physical quantities p, u, v and T are plotted in a cross-section located at one wavelength of the basic mode $A1$ away from the end ($x = 2\pi/\mathrm{Im}\,[K_{A1}]$). Further examples including also tubes of finite length are given in TH.

6.3. *Computer calculations of endlayers with rotational symmetry at low frequency*

In this section finally two examples of endlayers are presented for the case where the Stokes layer thickness $|\eta^{-1}|$ is equal to 1, i.e. where the flow away from the ends is of the Poiseuille type (more examples can be found in TH). Again a half-infinite tube is

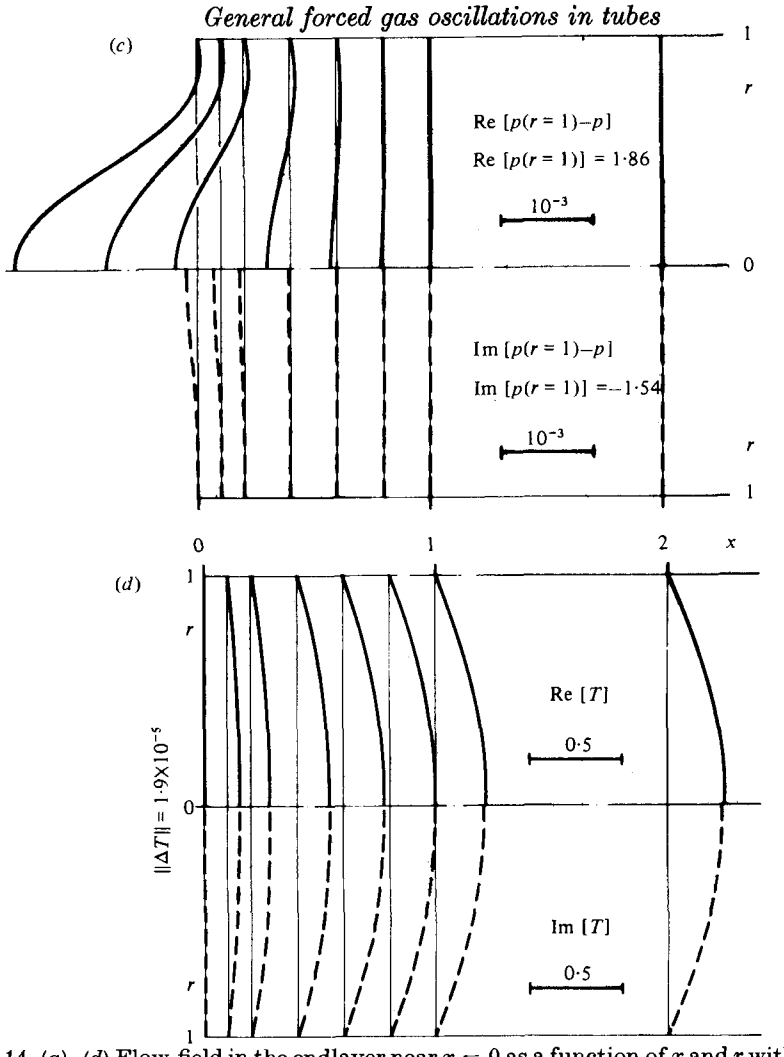

FIGURE 14. (*a*)–(*d*) Flow-field in the endlayer near $x = 0$ as a function of x and r with the excitation (PL) and $N_A = 21$, $L = \infty$, $\omega = 10^{-4}$, $\Lambda = 10^{-4}$, $\gamma = 1{\cdot}4$, $\sigma = 0{\cdot}71$, $\alpha = \frac{4}{3}$ (scales for the flow-variables are given in the diagrams).

considered because at this low frequency the interaction between the two endlayers of a finite tube is negligible unless the tube is very short ($L < 4$). In contrast to the resonance cases both end conditions, the oscillating plate (PL) and the plane piston (PI) defined by (5.11) and (5.12), have been used, as for a relatively thick boundary layer the non-linear effects in the corner between piston and tube wall do not significantly change the results of the linear theory according to the experimental evidence of Gerlach & Parker (1967). In the calculations for figures 14 and 15 the errors ar $x = 0$, i.e. the differences between the imposed end conditions and the calculated profiles at $x = 0$, contain primarily the highest modes $A21$ and $B21$, which are highly oscillatory in the radial direction and strongly damped in the x direction (cf. § 4.4). For better readability of the figures these oscillations have been smoothed out; to give an idea of the actual errors the envelopes of the oscillations at $x = 0$ are indicated by shaded

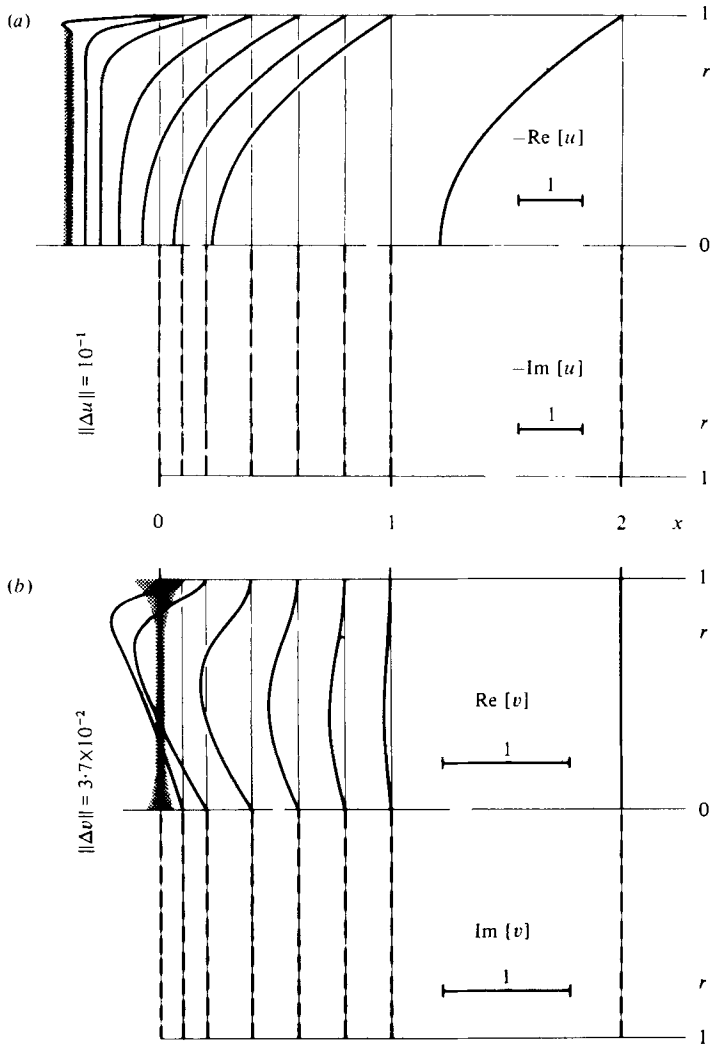

FIGURE 15(*a*, *b*). For legend see next page.

areas wherever they exceed the drawing accuracy of the smoothed profiles. In addition the error norms $-\|\Delta u\| = (u(x=0)-u_e,\ u(x=0)-u_e)^{\frac{1}{2}}$, $\|\Delta v\| = (v(x=0)-0,\ v(x=0)-0)^{\frac{1}{2}}$, etc. – are listed on the figures.

This work was prepared as a Ph.D. thesis under the direction of Prof. Nikolaus Rott. The author wishes also to acknowledge many helpful discussions with Prof. Eduard Stiefel.

Appendix. The general eigenfunctions

The eigenfunctions are obtained by eliminating three of the four constants C_v, C_t, C_u, C_w in the solutions of § 3 by use of the boundary conditions (2.13) at $r = 1$. To avoid singularities in the eigenfunctions it turns out that for each band a specific

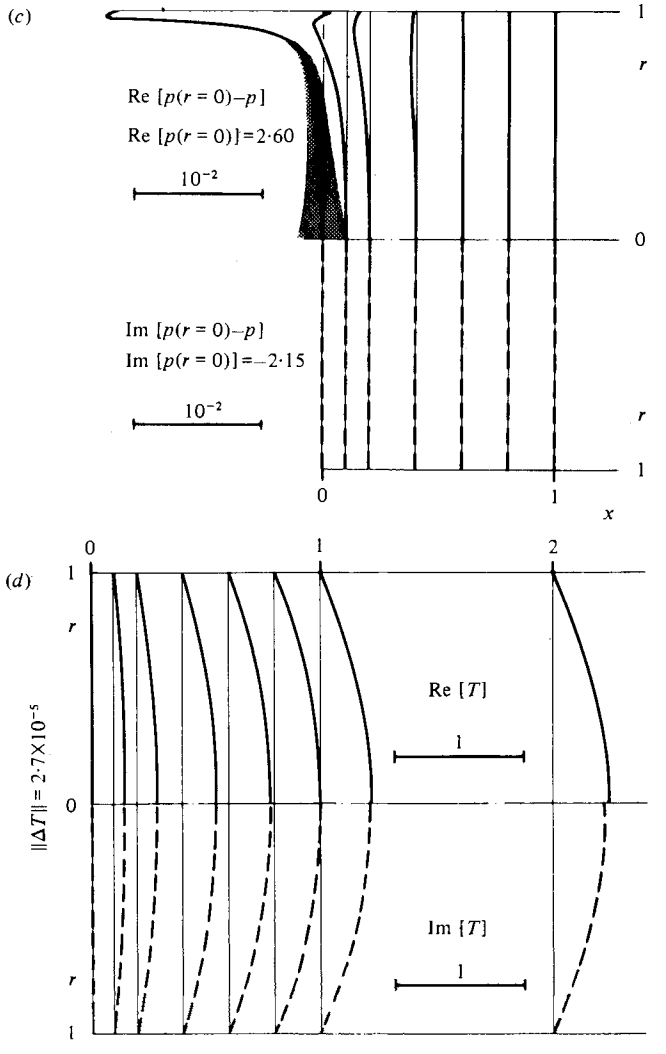

FIGURE 15. (*a*)–(*d*) Flow-field in the endlayer near $x = 0$ as a function of x and r with the excitation (*PI*) and $N_A = 21$, $L = \infty$, $\omega = 10^{-4}$, $\Lambda = 10^{-4}$, $\gamma = 1{\cdot}4$, $\sigma = 0{\cdot}71$, $\alpha = \frac{4}{3}$ (scales for the flow-variables are given in the diagrams).

natural amplitude has to be taken as independent amplitude in the elimination process.

First the *A-band* eigenfunctions are listed whereby the damped (index $-$) solutions have been recovered from the exponentially growing (index $+$) solutions proportional to $\exp(+Kx)$ through the symmetry relation of § 4.2. For numerical purposes the natural A-band amplitude C_v is normalized as follows:

$$\left.\begin{aligned} C^{+}_{An} &= C_v \frac{2^{\frac{1}{2}}}{K_{An} J_m(M_{v,An})} \exp[-K_{An}L] \quad \text{(tube length } L\text{)}, \\ C^{-}_{An} &= C_v \frac{2^{\frac{1}{2}}}{K_{An} J_m(M_{v,An})}. \end{aligned}\right\} \tag{A 1}$$

With this normalization the A-band eigenfunctions are given by the following expressions in which a prime denotes the derivative with respect to the argument:

$$
\left.\begin{aligned}
&T^+_{An} = C^+_{An}\,\hat{T}_{An}(r)\exp\left[-K_{An}(L-x)+im\theta+i\omega t\right],\\
&T^-_{An} = -C^-_{An}\,\hat{T}_{An}(r)\exp\left[-K_{An}x+im\theta+i\omega t\right],\\
&\hat{T}_{An}(r) = 2^{\frac{1}{2}}\frac{\Omega_v}{K_{An}}\left\{\frac{J_m(M_{v,An}r)}{J_m(M_{v,An})}-\frac{J_m(M_{t,An}r)}{J_m(M_{t,An})}\right\},\\
&u^+_{An} = C^+_{An}\,\hat{u}_{An}(r)\exp\left[-K_{An}(L-x)+im\theta+i\omega t\right],\\
&u^-_{An} = C^-_{An}\,\hat{u}_{An}(r)\exp\left[-K_{An}x+im\theta+i\omega t\right],\\
&\hat{u}_{An}(r) = 2^{\frac{1}{2}}\left\{\frac{J_m(M_{v,An}r)}{J_m(M_{v,An})}-\frac{\Omega_v}{\Omega_t}\frac{J_m(M_{t,An}r)}{J_m(M_{t,An})}-\left(1-\frac{\Omega_v}{\Omega_t}\right)\frac{J_m(M_{u,An}r)}{J_m(M_{u,An})}\right\},\\
&v^+_{An} = C^+_{An}\,\hat{v}_{An}(r)\exp\left[-K_{An}(L-x)+im\theta+i\omega t\right],\\
&v^-_{An} = -C^-_{An}\,\hat{v}_{An}(r)\exp\left[-K_{An}x+im\theta+i\omega t\right],\\
&\hat{v}_{An}(r) = 2^{\frac{1}{2}}\frac{M_{v,An}}{K_{An}}\left\{\frac{J'_m(M_{v,An}r)}{J_m(M_{v,An})}-\frac{\Omega_v}{\Omega_t}\frac{M_{t,An}}{M_{v,An}}\frac{J'_m(M_{t,An}r)}{J_m(M_{t,An})}\right.\\
&\qquad\qquad-\left(1-\frac{\Omega_v}{\Omega_t}\right)\frac{K^2_{An}}{M_{v,An}M_{u,An}}\frac{J'_m(M_{u,An}r)}{J_m(M_{u,An})}\\
&\qquad\qquad\left.+\left(1-\frac{\Omega_v}{\Omega_t}\right)\frac{K^2_{An}-M^2_{u,An}}{M_{v,An}M^3_{u,An}}\frac{m^2}{r}\frac{J_m(M_{u,An}r)}{J'_m(M_{u,An})}\right\},\\
&w^+_{An} = C^+_{An}\,\hat{w}_{An}(r)\exp\left[-K_{An}(L-x)+im\theta+i\omega t\right],\\
&w^-_{An} = -C^-_{An}\,\hat{w}_{An}(r)\exp\left[-K_{An}x+im\theta+i\omega t\right],\\
&\hat{w}_{An}(r) = 2^{\frac{1}{2}}\frac{im}{K_{An}}\left\{\frac{1}{r}\frac{J_m(M_{v,An}r)}{J_m(M_{v,An})}-\frac{\Omega_v}{\Omega_t}\frac{1}{r}\frac{J_m(M_{t,An}r)}{J_m(M_{t,An})}\right.\\
&\qquad\qquad-\left(1-\frac{\Omega_v}{\Omega_t}\right)\frac{K^2_{An}}{M^2_{u,An}}\frac{1}{r}\frac{J_m(M_{u,An}r)}{J_m(M_{u,An})}\\
&\qquad\qquad\left.+\left(1-\frac{\Omega_v}{\Omega_t}\right)\frac{K^2_{An}-M^2_{u,An}}{M^2_{u,An}}\frac{J'_m(M_{u,An}r)}{J'_m(M_{u,An})}\right\},\\
&p^+_{An} = C^+_{An}\,\hat{p}_{An}(r)\exp\left[-K_{An}(L-x)+im\theta+i\omega t\right],\\
&p^-_{An} = -C^-_{An}\,\hat{p}_{An}(r)\exp\left[-K_{An}x+im\theta+i\omega t\right],\\
&\hat{p}_{An}(r) = \frac{2^{\frac{1}{2}}}{K_{An}}\left\{\left[-i\omega+\Lambda\alpha(K^2_{An}-M^2_{v,An})\right]\frac{J_m(M_{v,An}r)}{J_m(M_{v,An})}\right.\\
&\qquad\qquad\left.-\frac{\Omega_v}{\Omega_t}\left[-i\omega+\Lambda\alpha(K^2_{An}-M^2_{t,An})\right]\frac{J_m(M_{t,An}r)}{J_m(M_{t,An})}\right\},\\
&\rho^+_{An} = C^+_{An}\,\hat{\rho}_{An}(r)\exp\left[-K_{An}(L-x)+im\theta+i\omega t\right],\\
&\rho^-_{An} = -C^-_{An}\,\hat{\rho}_{An}(r)\exp\left[-K_{An}x+im\theta+i\omega t\right],\\
&\hat{\rho}_{An}(r) = -\frac{2^{\frac{1}{2}}}{i\omega K_{An}}\left\{(K^2_{An}-M^2_{v,An})\frac{J_m(M_{v,An}r)}{J_m(M_{v,An})}\right.\\
&\qquad\qquad\left.-\frac{\Omega_v}{\Omega_t}(K^2_{An}-M^2_{t,An})\frac{J_m(M_{t,An}r)}{J_m(M_{t,An})}\right\},
\end{aligned}\right\}\qquad\text{(A 2)}
$$

Ω_v, Ω_t defined by (3.6), M_u (Re $[M_u] \geqslant 0$) defined by (3.4) and M_v, M_t defined by (3.9) and (3.10).

With C_u as independent *B-band* amplitude it follows immediately that the solution $M_{u,B1} = 0$ of the eigenvalue equation (4.1) for $(m,n) = (0,1)$ *represents the trivial solution* (cf. § 4.4) which has been overlooked by Scarton & Rouleau (1973). If in this case l'Hopital's rule is applied to the *A*-band expressions (A 2) then the resulting 'eigenfunctions' violate either the boundary conditions or the basic equations. For $(m,n) \neq (0,1)$ on the other hand the expressions (A 2) are appropriate also for the *B*-band.

The natural amplitude of the *C-band* is analogously found to be C_t. By this choice singularities are avoided when γ is set equal to 1. With the normalizations (A 3) the expressions (A 4) are then readily derived.

$$\left.\begin{aligned} C^+_{Cn} &= C_t \frac{2^{\frac{1}{2}}}{J'_m(M_{t\,Cn})} \exp(-K_{Cn}L), \\ C^-_{Cn} &= C_t \frac{2^{\frac{1}{2}}}{J'_m(M_{t,Cn})}. \end{aligned}\right\} \tag{A 3}$$

$$\left.\begin{aligned}
T^+_{Cn} &= C^+_{Cn}\hat{T}_{Cn}(r)\exp[-K_{Cn}(L-x)+im\theta+i\omega t], \\
T^-_{Cn} &= -C^-_{Cn}\hat{T}_{Cn}(r)\exp[-K_{Cn}x+im\theta+i\omega t], \\
\hat{T}_{Cn}(r) &= 2^{\frac{1}{2}}\left\{-\frac{J_m(M_{t,Cn})}{J'_m(M_{t,Cn})}\frac{J_m(M_{v,Cn}r)}{J_m(M_{v,Cn})}+\frac{J_m(M_{t,Cn}r)}{J'_m(M_{t,Cn})}\right\}, \\
u^+_{Cn} &= C^+_{Cn}\hat{u}_{Cn}(r)\exp[-K_{Cn}(L-x)+im\theta+i\omega t], \\
u^-_{Cn} &= C^-_{Cn}\hat{u}_{Cn}(r)\exp[-K_{Cn}x+im\theta+i\omega t], \\
\hat{u}_{Cn}(r) &= 2^{\frac{1}{2}}\frac{K_{Cn}}{\Omega_v}\left\{-\frac{J_m(M_{t,Cn})}{J'_m(M_{t,Cn})}\frac{J_m(M_{v,Cn}r)}{J_m(M_{v,Cn})}+\frac{\Omega_v}{\Omega_t}\frac{J_m(M_{t,Cn}r)}{J'_m(M_{t,Cn})}\right. \\
&\qquad \left.+\left(1-\frac{\Omega_v}{\Omega_t}\right)\frac{J_m(M_{t,Cn})}{J'_m(M_{t,Cn})}\frac{J_m(M_{u\,Cn}r)}{J_m(M_{u,Cn})}\right\}, \\
v^+_{Cn} &= C^+_{Cn}\hat{v}_{Cn}(r)\exp[-K_{Cn}(L-x)+im\theta+i\omega t], \\
v^-_{Cn} &= -C^-_{Cn}\hat{v}_{Cn}(r)\exp[-K_{Cn}x+im\theta+i\omega t], \\
\hat{v}_{Cn}(r) &= \frac{2^{\frac{1}{2}}}{\Omega_v}\left\{-M_{v,Cn}\frac{J_m(M_{t,Cn})}{J'_m(M_{t,Cn})}\frac{J'_m(M_{v,Cn}r)}{J_m(M_{v,Cn})}+\frac{\Omega_v}{\Omega_t}M_{t,Cn}\frac{J'_m(M_{t,Cn}r)}{J'_m(M_{t,Cn})}\right. \\
&\qquad +\left(1-\frac{\Omega_v}{\Omega_t}\right)\frac{K^2_{Cn}}{M_{u,Cn}}\frac{J_m(M_{t,Cn})}{J'_m(M_{t,Cn})}\frac{J'_m(M_{u\,Cn}r)}{J_m(M_{u,Cn})} \\
&\qquad \left.-\left(1-\frac{\Omega_v}{\Omega_t}\right)\frac{K^2_{Cn}-M^2_{u,Cn}}{M^3_{u,Cn}}\frac{J_m(M_{t,Cn})}{J'_m(M_{t,Cn})}\frac{m^2}{r}\frac{J_m(M_{u,Cn}r)}{J'_m(M_{u,Cn})}\right\}, \\
w^+_{Cn} &= C^+_{Cn}\hat{w}_{Cn}(r)\exp[-K_{Cn}(L-x)+im\theta+i\omega t], \\
w^-_{Cn} &= -C^-_{Cn}\hat{w}_{Cn}(r)\exp[-K_{Cn}x+im\theta+i\omega t], \\
\hat{w}_{Cn}(r) &= 2^{\frac{1}{2}}\frac{im}{\Omega_v}\left\{-\frac{J_m(M_{t,Cn})}{J'_m(M_{t,Cn})}\frac{1}{r}\frac{J_m(M_{v,Cn}r)}{J_m(M_{v,Cn})}+\frac{\Omega_v}{\Omega_t}\frac{1}{r}\frac{J_m(M_{t,Cn}r)}{J'_m(M_{t,Cn})}\right. \\
&\qquad +\left(1-\frac{\Omega_v}{\Omega_t}\right)\frac{K^2_{Cn}}{M^2_{u,Cn}}\frac{J_m(M_{t,Cn})}{J'_m(M_{t,Cn})}\frac{1}{r}\frac{J_m(M_{u,Cn}r)}{J_m(M_{u,Cn})} \\
&\qquad \left.-\left(1-\frac{\Omega_v}{\Omega_t}\right)\frac{K^2_{Cn}-M^2_{u,Cn}}{M^2_{u,Cn}}\frac{J_m(M_{t,Cn})}{J'_m(M_{t,Cn})}\frac{J'_m(M_{u\,Cn}r)}{J'_m(M_{u,Cn})}\right\},
\end{aligned}\right\} \tag{A 4}$$

$$
\left.\begin{aligned}
p^{+}_{Cn} &= C^{+}_{Cn}\,\hat{p}_{Cn}(r)\exp\left[-K_{Cn}(L-x)+im\theta+i\omega t\right],\\
p^{-}_{Cn} &= -C^{-}_{Cn}\,\hat{p}_{Cn}(r)\exp\left[-K_{Cn}x+im\theta+i\omega t\right],\\
\hat{p}_{Cn}(r) &= \frac{2^{\frac{1}{2}}}{\Omega_v}\left\{-\left[-i\omega+\Lambda\alpha(K^2_{Cn}-M^2_{v,Cn})\right]\frac{J_m(M_{t,Cn})}{J'_m(M_{t,Cn})}\,\frac{J_m(M_{v,Cn}r)}{J_m(M_{v,Cn})}\right.\\
&\qquad\left.+\frac{\Omega_v}{\Omega_t}\left[-i\omega+\Lambda\alpha(K^2_{Cn}-M^2_{t,Cn})\right]\frac{J_m(M_{t,Cn}r)}{J'_m(M_{t,Cn})}\right\},\\
\rho^{+}_{Cn} &= C^{+}_{Cn}\,\hat{\rho}_{Cn}(r)\exp\left[-K_{Cn}(L-x)+im\theta+i\omega t\right],\\
\rho^{-}_{Cn} &= -C^{-}_{Cn}\,\hat{\rho}_{Cn}(r)\exp\left[-K_{Cn}x+im\theta+i\omega t\right],\\
\hat{\rho}_{Cn}(r) &= \frac{2^{\frac{1}{2}}}{i\omega\Omega_v}\left\{(K^2_{Cn}-M^2_{v,Cn})\frac{J_m(M_{t\,Cn})}{J'_m(M_{t,Cn})}\,\frac{J_m(M_{v\,Cn}r)}{J_m(M_{v,Cn})}\right.\\
&\qquad\left.-\frac{\Omega_v}{\Omega_t}(K^2_{Cn}-M^2_{t,Cn})\frac{J_m(M_{t,Cn}r)}{J'_m(M_{t,Cn})}\right\}.
\end{aligned}\right\}
$$

In the *D-band* the case $m = 0$ has to be considered separately. The solution has already been found in § 4.2 to be a pure w-solution which for completness is again listed in normalized form.

For $m = 0$:

$$
\left.\begin{aligned}
T^{\pm}_{Dn} &= 0,\\
u^{\pm}_{Dn} &= 0,\\
v^{\pm}_{Dn} &= 0,\\
w^{+}_{Dn} &= C^{+}_{Dn}\,\hat{w}_{Dn}(r)\exp\left[-K_{Dn}(L-x)+i\omega t\right],\\
w^{-}_{Dn} &= C^{-}_{Dn}\,\hat{w}_{Dn}(r)\exp\left[-K_{Dn}x+i\omega t\right],\\
\hat{w}_{Dn}(r) &= 2^{\frac{1}{2}}\frac{J_1(j_{1,n}r)}{J_0(j_{1,n})},\\
p^{\pm}_{Dn} &= 0,\\
\rho^{\pm}_{Dn} &= 0.
\end{aligned}\right\}
\tag{A 5}
$$

For $m > 0$ the expressions (A 2) are appropriate also for the D-band, whereby an additional normalization (A 6) might be useful:

$$
C^{\pm}_{Dn} = C^{\pm}_{An}\frac{J'_m(M_{u,Dn})}{J_m(M_{u,Dn})}.
\tag{A 6}
$$

REFERENCES

Abramowitz, M. & Stegun, I. A. 1969 *Handbook of Mathematical Functions*. 5th ed. Dover.

Bergh, H. & Tijdeman, H. 1965 Theoretical and experimental results for the dynamic response of pressure measuring systems. Nat. Aero. Astro. Res. Inst. Amsterdam. *NLR-TR* F. 238.

Chester, W. 1964 Resonant oscillations in closed tubes. *J. Fluid Mech.* **18**, 44–66.

Detournay, P. & Piessens, R. 1971 Zeros of Bessel functions and zeros of cross-products of Bessel functions. Appl. Math. Div., Katholieke Universiteit Leuven (Netherland), *Report TW* 7.

Ellacott, S. & Williams, J. 1976 Linear Chebyshev approximation in the complex plane using Lawson's algorithm. *Math. of Computation*, **30**, 35–44.

Fitz-Gerald, J. M. 1972 Plasma motions in narrow capillary tubes. *J. Fluid Mech.* **51**, 463–476.

GERLACH, C. R. & PARKER, J. D. 1967 Wave propagation in viscous fluid lines including higher mode effects. *J. of Basic Ing., Trans. A.S.M.E.* D, **89**, 782–788.

HUERRE, P. & KARAMCHETI, K. 1976 Effects of friction and heat conduction on sound propagation in ducts. Stanford University *J.I.A.A. TR*-4.

IBERALL, A. S. 1950 Attenuation of oscillatory pressures in instrument lines. *J. Res. National Bur. Stand.* **45**, 85.

KANTOROVICH, L. & KRYLOV, V. 1964 *Approximate Methods of Higher Analysis.* New York: Interscience.

KELLER, J. 1975 Subharmonic non-linear acoustic resonances in closed tubes. *Z. angew. Math. Phys.* **26**, 395–405.

KELLER, J. 1976 Resonant oscillations in closed tubes: the solution of Chester's equation. *J. Fluid Mech.* **77**, 279–304.

KIRCHHOFF, G. 1868 Ueber den Einfluss der Wärmeleitung in einem Gase auf die Schallbewegung. *Pogg. Ann.* **134**, 177.

MERKLI, P. & THOMANN, H. 1975 Transition to turbulence in oscillating pipe flow. *J. Fluid Mech.* **68**, 567–575.

MONKEWITZ, P. A. 1977 (TH) Die vollständige lineare Behandlung von erzwungenen Gasschwingungen in Rohren. Ph.D. thesis no. 5900, ETH Zürich.

NIRENBERG, L. 1955 Remarks on strongly elliptic partial differential equations. *Comm. Pure Appl. Math.* **8**, 648–674.

RAYLEIGH, LORD 1945 *Theory of Sound.* 2nd ed. Dover.

ROTT, N. 1969 Damped and thermally driven acoustic oscillations in wide and narrow tubes. *Z. angew. Math. Phys.* **20**, 230–243.

SCARTON, H. A. 1970 Waves and stability in viscous and inviscid compressible liquids contained in rigid and elastic tubes by the method of Eigenvalleys (Vols. I–III). Ph.D. Thesis, Carnegie-Mellon Univ. Nr. 70–18,029 University Microfilms Inc., Ann Arbor, Michigan.

SCARTON, H. A. & ROULEAU, W. T. 1973 Axisymmetric waves in compressible Newtonian liquids contained in rigid tubes: steady-periodic mode shapes and dispersion by the method of Eigenvalleys. *J. Fluid Mech.* **58**, 595–621.

SCHWARZ, H. R., RUTISHAUSER, H. & STIEFEL, E. 1972 *Matrizen-Numerik.* Teubner Stuttgart, 2. Aufl.

SERGEEV, S. I. 1966 Fluid oscillations in pipes at moderate *Re*-numbers. *Fluid Dynamics*, **1**, 121–122.

TIJDEMAN, H. 1975 On the propagation of sound waves in cylindrical tubes. *J. Sound Vib.* **39**, 1–33.